POLITECNICO DI TORINO

Master's Degree in Biomedical Engineering

Master's Degree Thesis

User-Adapted Neurostimulation via Binaural Beats for Stress Reduction

Supervisors

Prof. Luca Mesin

Ing. Matteo Raggi

Candidate

Stefania Chiri

Academic Year 2023-2024

Abstract

Acute stress is a physiological and psychological condition that manifests when the demands of either a real-life situation or a cognitive task exceed the resources we have available to cope. If not treated, acute stress can turn into chronic, resulting in serious physical and psychological issues, including cardiovascular diseases, anxiety, and decreased productivity. Furthermore, it may have significant economic consequences, such as increased absenteeism in the workplace. This project aims to develop a real-time algorithm for stress detection and reduction by exploiting binaural beats. Binaural beats are an auditory stimulation that occurs when two tones with a slight frequency mismatch are presented separately to each ear. This results in a perceived signal, reconstructed in our brain, with an amplitude that oscillates at a frequency equal to the difference between the two tones. While existing literature is mainly focused on fixed stimulation approaches with contradictory results, this thesis aims to evaluate whether an adaptive stimulation approach, piloted by a stress detection algorithm, can effectively reduce stress. In other words, the goal is to identify a personalised stimulation frequency in the theta band (4 to 8 Hz) to induce relaxation. An experimental protocol to induce acute mental stress was designed, considering as stressor a mental arithmetic task with a limited time to provide the answers. In addition, different questionnaires were filled out by the volunteers to analyse the psychological responses and the affective conditions of the participants (18 undergraduate students). The technique was compared with fixed and no-stimulation conditions. For this study, the PolarH10 chest strap was used as a device for data collection. The features from both the electrocardiogram (ECG) and the breath rate, indirectly estimated from the ECG, were considered for our method. By doing so, the connectivity between respiratory activity and the heart is considered. Results show that the experimental protocol was capable of inducing stress in the participants. Indeed, the heart rate is higher during the task than during the baseline ($p<0.001$), i.e., a period of 2 minutes before the beginning of the cognitive task,

which lasts 4 minutes. Furthermore, we detected a significantly lower value of the regressor's output (p=0.022) when comparing the adapted stimulation approach with the fixed stimulation condition. No statistical differences were detected in terms of accuracy and reaction times in the cognitive tasks, indicating no learning effect by the participants. Future studies are required to assess the goodness of the proposal, both considering additional candidates and different experimental conditions.

Contents

List of Figures

List of Tables

Chapter 1

Introduction

This chapter aims to provide the theoretical framework necessary for comprehending the work conducted. Specifically, it explores topics ranging from physiology, focusing on the stress response and cardiac function, to biomedical signal processing, artificial intelligence algorithms, and neurostimulation. The chapter concludes with an analysis of the current state of the art on the topics discussed.

1.1 Overview

Acute mental stress is a widespread issue affecting many people nowadays. Although it is a psychological condition, it may lead to cardiovascular diseases [2], hypertension [3], insomnia [4], and a weakened immune system [5]. If not treated, acute stress can turn into chronic. Stress is the main cause of the development of mental disorders such as anxiety, depression, and burnout [6]. It can influence the quality of life, negatively affecting productivity, concentration, and performance, both at work and in school. Mismanaged stress has a significant economic impact, both for individuals and organizations. It can lead to increased absenteeism and higher healthcare costs [7]. For these reasons, it is useful to study how stress affects the physiology of an individual, and how it can be reduced.

Stress can be defined as the perturbation of physiological systems, such as the autonomic nervous system (ANS) and the endocrine system, whose job is to maintain the homeostasis [8]. Stressors, indeed, affect an individual's homeostasis; the brain

evaluates them for their importance according to previous experience and current life [2]. Stress occurs when the environmental demand exceeds the natural regulatory capacity of an organism to cope with it [9].
The main issue related to stress is the lack of a commonly shared definition of it [10]. Currently, the gold-standard for stress assessment is the cortisol response magnitude. During a stressful experience, the increase in cortisol is directly associated with the level of stress [11]. However, recent studies have demonstrated that Heart Rate Variability (HRV) is a reliable index of stress [10], while others also use QT variability and breath rate as indicators [3].

1.2 Physiological Stress Response

The two main pathways by which psychological stress impacts the body are the hypothalamus-pituitary-adrenal (HPA) axis and the autonomic nervous system (ANS), that are higly interconnected and coordinated. The ANS is divided into sympathetic nervous system (SNS) and parasympathetic nervous system (PNS). Under stress conditions, the activity of the SNS predominates over the PNS, triggering the so-called "fight or flight" response. This reaction is specifically mediated by the sympatho-adrenomedullary (SAM) system, which rapidly regulates cardiovascular and metabolic activity to prepare the body to face a potential threat [8]. The SAM system responds more quickly (within seconds) compared to the HPA axis, which takes minutes to have an effect [3].

1.2.1 HPA Axis

The activation of the HPA axis causes the secretion of glucocorticoids, including cortisol. During a stress response, the amygdala triggers the hypothalamus to produce corticotropin-releasing hormone (CRH), which then prompts the pituitary gland to release adrenocorticotropic hormone (ACTH) into the bloodstream. This, in turn, stimulates cortisol production in the adrenal cortex (Fig. 1.1). The rise in cortisol helps the body access additional energy by promoting liver gluconeogenesis and breaking down tissue proteins and fat stores. Cortisol enters saliva by diffusing

from blood plasma. Several inhibitory feedback loops to the pituitary gland and hypothalamus regulate these secretion processes [3].

1.2.2 SAM System

The SAM system responds to stress by secreting catecholamines (epinephrine and norepinephrine). The hypothalamus triggers the brainstem, which subsequently activates the efferent sympathetic pathways. In this way, norepinephrine is released at sympathetic neuroeffector junctions, and the secretion of epinephrine in the adrenal medulla is stimulated (Fig. 1.1). The whole stress response mechanism is coordinated by the brainstem, which provides feedback to cortex, hippocampus, and amygdala. The activation of this system causes an increase in heart rate, breath rate, and miocardial contractility, accompanied by peripheral vasoconstriction and vasodilation in skeletal muscle and in the heart. Other consequences are pupillary dilation, bronchodilation, increased sweat gland activity, and inhibition of digestive activity. Moreover, the flow rate of saliva decreases, while its concentration of α-amylase increases. However, the concentration of this protein and the flow rate are regulated by PNS as well, complicating the assessment of stress levels using this measure [3].

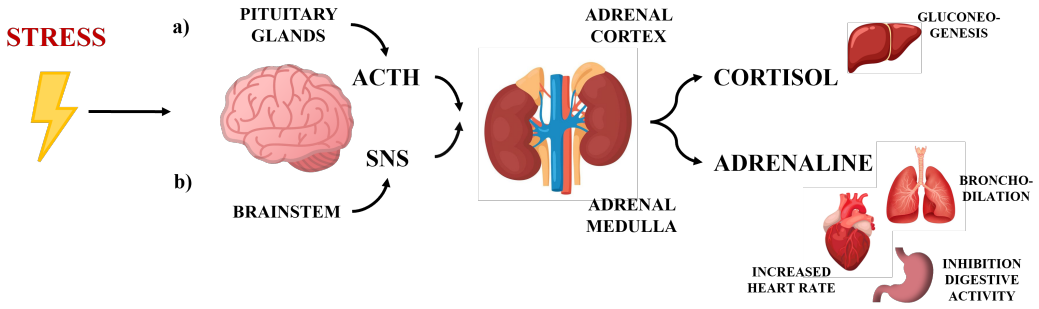

Fig. 1.1 Hypothalamic–pituitary–adrenal axis (a) and sympatho-adrenomedullary system (b).

To sum up, the activity of these two pathways can be measured by cortisol levels for the HPA axis, and by HRV for the SAM system. Measuring cortisol levels would involve taking multiple samples over time (from blood, saliva, or hair [12]), making the procedure challenging for real-time applications [13]. As a consequence of that, to evaluate stress levels in this work, HRV and other ECG signal-derived data are employed.

1.3 Heart

1.3.1 Anatomy

The heart is a muscular organ located centrally in the chest behind the sternum in a space called mediastinum. It is composed of four chambers: the right and left atria, the upper chambers, and the right and left ventricles, the lower chambers, respectively (Fig. 1.2). The right atrium and ventricle are referred to as the right heart, while the left atrium and ventricle together constitute the left heart [14]. Right and left heart are separated by the cardiac septum. The upper part of the heart is called the base, while the lower part of the heart is called the apex. Atria receive continuously blood from the various districts of the body, while ventricles are responsible for pumping it out and sending it to the other areas of the body.

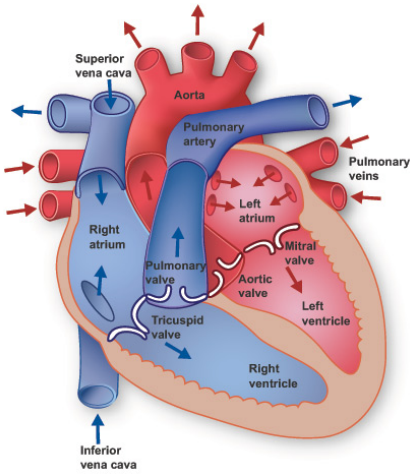

Fig. 1.2 Anatomy of the heart.

1.3.2 Innervation

The heart is innervated by the accelerans and the vagus nerves, which are responsible for the sympathetic and the parasympathetic response, respectively. Sympathetic efferences of the ANS release norepinephrine as the main neurotransmitter, that stimulates β-adrenergic receptors, thereby increasing cardiac contractility and heart rate [15]. The SNS primarily influences the ventricular muscles, and also increases the frequency of excitation, conduction velocity, and excitability of the sinoatrial

(SA) node [10]. Parasympathetic efferences, on the other hand, release acetylcholine (ACH), that binds with muscarinic receptors, and has an opposite effect to that of the norepinephrine [15]. The PNS mainly affects the SA and atrioventricular (AV) nodes, leading to a reduction in heart rate. Due to the high concentration of acetylcholinesterase in the SA node, the effect of vagal impulses is brief, as acetylcholine is rapidly hydrolyzed. At rest, parasympathetic activity predominates over the sympathetic one [10].

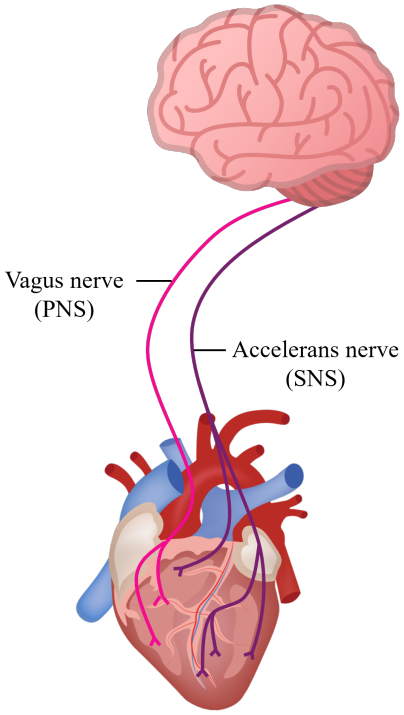

Fig. 1.3 Innervation of the heart: sympathetic and parasympathetic ways.

1.3.3 Cardiac Conduction System

The heart muscle is composed by cardiomyocytes, that have unique contractile properties and structures. They facilitate the cell-to-cell communication through intercalated discs. These discs minimize internal resistance, allowing action potentials to propagate rapidly across the heart via electrically charged particles known as ions. This organ works as a coordinated syncytium, with quick, synchronized

contractions that drive the pumping of blood. To produce each heartbeat, the heart relies on electrochemical gradients and on the generation of contractile force [15].

To make the heart contract autonomously, cardiac tissue has pacemaker cells. These cells are located in the SA node, which generates the rhythm, and in the AV node, which ensures that the ventricles contract following the atria.

The electrical signal generates in the SA node, and then propagates through the internodal pathways to the AV node, as previously described. The propagation of the potential to the AV node leads to the depolarization of the atria. The depolarization of the ventricles occurs thanks to the intraventricular conduction system, consisting of the bundle of His, which divides into the right and left branches. The right branch continues the course of the bundle of His along the septum, while the left branch, which is thicker, perforates the interventricular septum, that in turn branch out into the Purkinje fibers (Fig. 1.4). Following depolarization, repolarization occurs. In the case of the atria, the first cells to depolarize are the first to repolarize, while in the ventricles, the first cells to depolarize are the last to undergo the repolarization process. This is because action potentials are not all of equal duration [16].

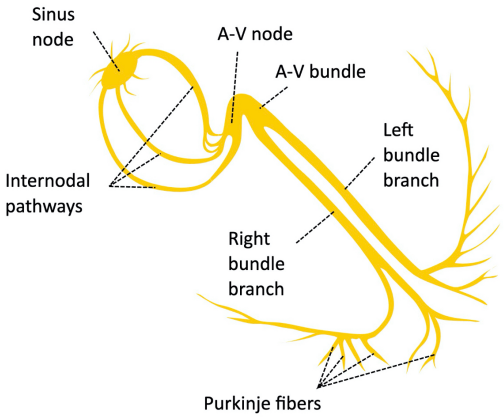

Fig. 1.4 Cardiac conduction system.

Due to the periodic depolarizations and repolarizations of the cardiac tissue, electrical currents are spread from the heart throughout the body surface. By placing electrodes on the skin, it is possible to record the cardiac activity acquiring the electrocardiographic (ECG) signal.

1.3.4 ECG Signal

When a myocardial fiber is excited, an action potential propagates along it. Each individual cardiac fiber behaves like a dipole during the action potential, so the electrical activity of each myocardial fiber can be represented by an electric vector (or dipole vector). By acquiring the ECG signal, the entire myocardial activity is recorded. Since the heart is a muscular syncytium, it can be modeled as a single dipole, characterized by its own vector, known as the cardiac vector [16].

The direction of the cardiac vector varies over time because the charges shift relative to the cardiac surface during depolarization. The signal that is acquired is a spatial reconstruction of the instantaneous electrical vector. The Einthoven triangle is a theoretical model that helps to understand how the limb leads reflect the heart's electrical activity from different angles, providing essential information for ECG interpretation. With this model, the projection of the cardiac vector can be observed onto three segments formed by the connection between two electrodes, known as a bipolar lead [17].

In bipolar leads, electrodes are placed on the right wrist, on the left wrist, and on the left ankle. The electrodes arranged this way form an equilateral triangle, with the heart at its center (Fig. 1.5).

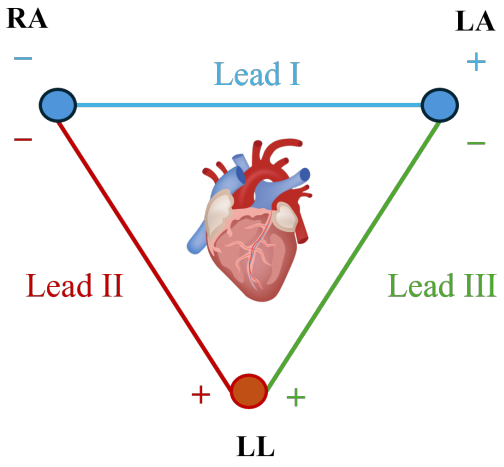

Fig. 1.5 Einthoven triangle.

With this configuration there are three limb leads:

- Lead I: measured between the positive electrode on the left arm (LA) and the negative electrode on the right arm (RA).

$$I = LA - RA$$

- Lead II: measured between the positive electrode on the left leg (LL) and the negative electrode on the RA.

$$II = LL - RA$$

- Lead III: measured between the positive electrode on the LL and the negative electrode on the LA.

$$III = LL - LA$$

1.3.5 Genesis of the Electrocardiogram

The signal is generated at the SA node and propagates along the adjacent cardiac cells. The first heart chambers to be depolarized are, therefore, the atria. The depolarization of the atria corresponds to the P wave on the electrocardiogram. At the end of this wave, with a delay of about 100 ms, the signal is generated at the AV node, which triggers the depolarization of the septum. This brief period, during which no signal is recorded, corresponds to the PQ segment.

The depolarization of the ventricles is represented by the QRS complex, which consists of the succession of the Q, R, and S waves. The Q wave corresponds to the depolarization of the septum, which begins with the left-side depolarization of the bundle of His. The signal propagates perpendicularly across the septum, continuing towards the right side, and then spreads towards the apex of the heart. The maximum signal amplitude is recorded when the cardiac vector is directed towards the left ventricle.

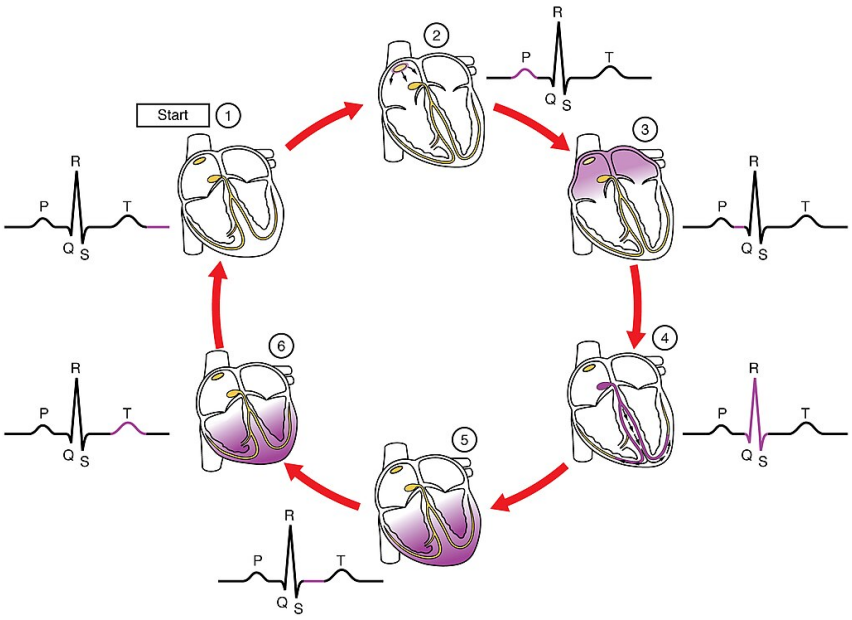

Fig. 1.6 Genesis of the waveforms within the electrocardiogram [1].

The ventricle has a more developed muscular wall, since it pumps blood throughout the systemic circulation, and therefore the potential has to overcome a greater resistance. The depolarization of the apex of the left ventricle corresponds to the peak of the R wave, followed by the S wave, which corresponds to the depolarization of the basal and posterior regions of the left ventricle.

Subsequently, the electrocardiogram shows an isoelectric segment (the ST segment), during which the ventricles return to rest. Finally, the last waveform that can be observed is the T wave, which corresponds to the repolarization of the ventricles. The repolarization of the atria, on the other hand, is not visible on the ECG tracing because it is obscured by the depolarization of the ventricles. Another interval that can be seen on the electrocardiogram is the QT interval, which represents the electrical systole, that is the time required for the depolarization and repolarization of the ventricles.

Table 1.1 shows the duration ranges of each of the electrocardiogram waveforms for a healthy person [18], while Fig. 1.7 presents the full waveform of an ECG signal.

Table 1.1 Physiological ranges for a healthy subject.

Waveform	Duration (ms)
P wave	60-120
PQ segment	12-20
QRS complex	60-90
ST segment	230-460
T wave	100-250
QT interval	350-440

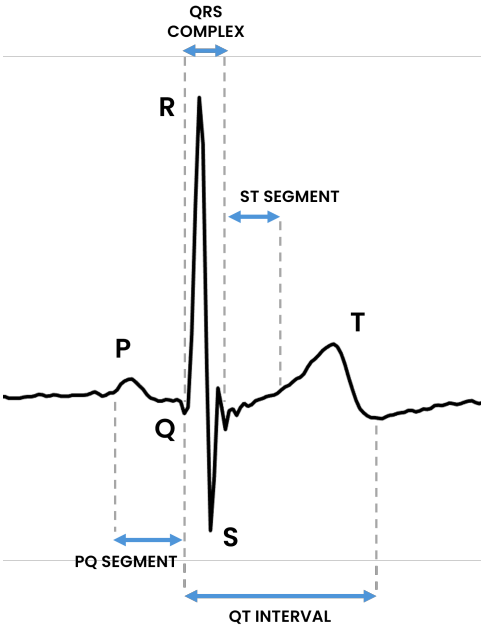

Fig. 1.7 Electrocardiogram of a healthy subject.

1.3.6 EDR Signal

The ECG waveform morphology changes with respiration due to the rotation of the electrical axis caused by chest movements during the respiratory cycle [19],[20].For this reason, it is possible to extract the respiratory signal from the ECG, obtaining the so called ECG-derived respiratory (EDR) signal. In this case the ECG should be acquired placing electrodes on the chest in order to detect the changes in thoracic impedance caused by respiration [21].

During inhalation, the apex of the heart is pushed toward the abdomen as the lungs fill and the diaphragm moves downward. Conversely, during exhalation, the apex of the heart is compressed toward the chest as the lungs empty and the diaphragm moves upward. Due to the anatomical changes in the heart's position within the chest during respiration, the angles of the mean QRS vector vary, which causes the amplitude changes in the ECG [21].

In the literature, other methods than those based on peak amplitude variation have been explored for extracting the respiratory signal from the ECG. Some of them are based on the respiratory sinus arrhythmia (RSA), i.e. the change of heart rate depending on the respiration. During inspiration, the sympathetic activity increases, thus increasing heart rate and resulting in a compressed QRS complex. During exhalation, on the other hand, the vagal tone increases; consequently, the heart rate decreases, and the QRS complex is more expanded [19],[22].

Another possibility is to extract the EDR signal using the area under the QRS complex [23] or the slope of the QRS complex [24]. However, in this work, the chosen method for respiratory signal extraction is based on the amplitude variation in the ECG.

1.4 Machine Learning Algorithms

As mentioned in the previous paragraphs, this project aims to identify a subject's stress levels based on their ECG. To achieve this, artificial intelligence algorithms are used, specifically, those of machine learning (ML). With ML, the computer learns and improves from experience without being explicitly programmed. The algorithm is provided with input features and learns to assign corresponding outputs during the training phase. Once the model is defined, it can be applied to new data. Various kinds of algorithm can be utilized depending on the nature of the data and the intended outcome. Based on the type of input data, the algorithms are classified into [25]:

- **Supervised**: the input have a label, which means that their true class is known. The algorithm learns to assign the data to the relative class.
- **Unsupervised**: the input does not have a label. These algorithms try to find some patterns within the data, assigning similar outputs to similar input data.

- **Reinforcement learning**: an agent learns to make decisions by interacting with an environment. The agent selects actions aimed at maximizing the total rewards accumulated over time. This algorithm learns from the consequences of actions.

Based on the intended outcome, ML algorithms can perform two tasks:

- **Classification**: the algorithm provides an integer number that indicates the class to which the input element belongs.
- **Regression**: the algorithm predicts a continuous numerical value according to the model that describes the relationship between input features and the target variable.

Two different supervised learning algorithms are explored in this work: the Random Forest (RF) regressor, and the Support Vector Machine regressor (SVR). Regression is preferred over classification because stress is not a discrete phenomenon; therefore, it should be analyzed using continuous target values [26].

1.4.1 Random Forest Regressor

RF is based on the decision tree algorithm. A decision tree is a graphical representation of choices and their outcomes, structured as a tree (Fig. 1.8). In this graph, nodes represent events or decisions, while the edges denote the decision rules or conditions. Each tree consists of nodes and branches, where each node represents an attribute of the group being classified, and each branch shows the possible values of that attribute [25]. RF utilizes multiple decision trees, since having a large number of trees improves learning and accuracy. RF uses bootstrap sampling for their construction [27]. This technique also helps to prevent overfitting and to increase the stability of the algorithm [25]. Random samples are drawn from the training data to construct the decision trees, and features are randomly chosen for splitting the nodes of these trees. This process of random data and feature selection is what gives the method its name, Random Forest. A RF model creates an ensemble of a number of trees, with the final prediction being the average of the predictions made by each individual decision tree [27].

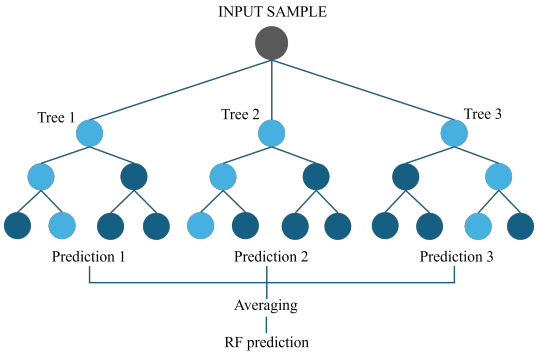

Fig. 1.8 Schematic representation of the RF algorithm.

1.4.2 Support Vector Regressor

The SVR algorithm aims to find a line (or a hyperplane in higher-dimensional spaces) so that most of the data points lie within a certain defined margin of error ε (Fig. 1.9). Points that fall outside this margin influence the model in a way that minimizes the overall error. Errors that fall within the ε range are penalized as zero. Only errors greater than ε are penalized, which helps the model focus on important deviations from the predicted values. The regularization parameter, C, controls the trade-off between achieving low errors on the training data and keeping the model as simple as possible. A higher value of C gives priority to minimizing training errors, while a smaller value allows more tolerance for errors to avoid overfitting. SVR can also use the kernel trick to transform the input data into a higher-dimensional space. This allows the algorithm to learn nonlinear relationships between input variables by finding a linear decision boundary in the transformed space. Common kernels include linear, polynomial, and radial basis function (RBF) kernels [27].

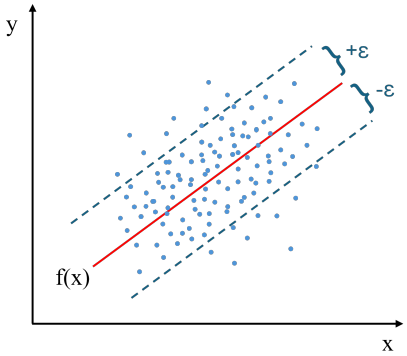

Fig. 1.9 Example of a SVR.

1.5 Binaural Beats

Binaural beats (BB) are a phenomenon related to the auditory system's ability to process phase differences between the two ears [28]. When two tones with a slight frequency mismatch are presented separately to each ear, a third tone, known as a binaural beat, is perceived within the head, oscillating at the absolute difference between the tones (Fig. 1.10) [29].

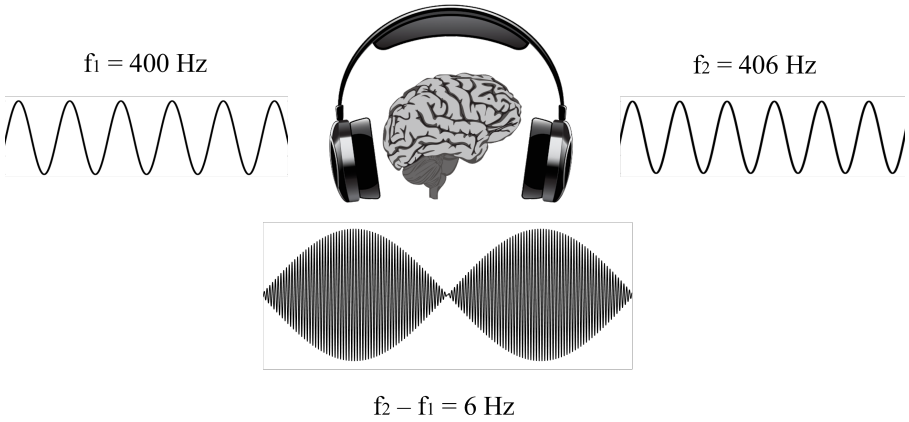

Fig. 1.10 Formation of the 6 Hz binaural beat.

This third tone is an auditory illusion, since it is not present acoustically, and, normally, the human auditory system would not perceive tones under 20 Hz. A BB can be produced by two pure tones that both have frequencies below 1500 Hz and differ by less than 40 Hz [30]. The tones are usually delivered through headphones to ensure that each ear is exposed to only one of the two frequencies [31].

The perception of BB arises from the superposition of afferent signals at a neural center connected to the cochlea of each ear, where the processing of low-frequency sound signals occurs. This neural center is located in the brainstem and consists of the superior olivary complexes, where the signals coming from each cochlea are integrated before reaching the auditory cortex. The two superior olivary nuclei are symmetrically positioned on each side of the brain, serving as termination points for nerve fibers from both ears (Fig. 1.11) [32].

The stimulus provided through BB generates a frequency-following response in the brain, leading to the phenomenon of brainwave entrainment, where cortical activity is induced to oscillate at the stimulation frequency or at its multiples. The frequency used for stimulation is selected based on the intended outcome, targeting

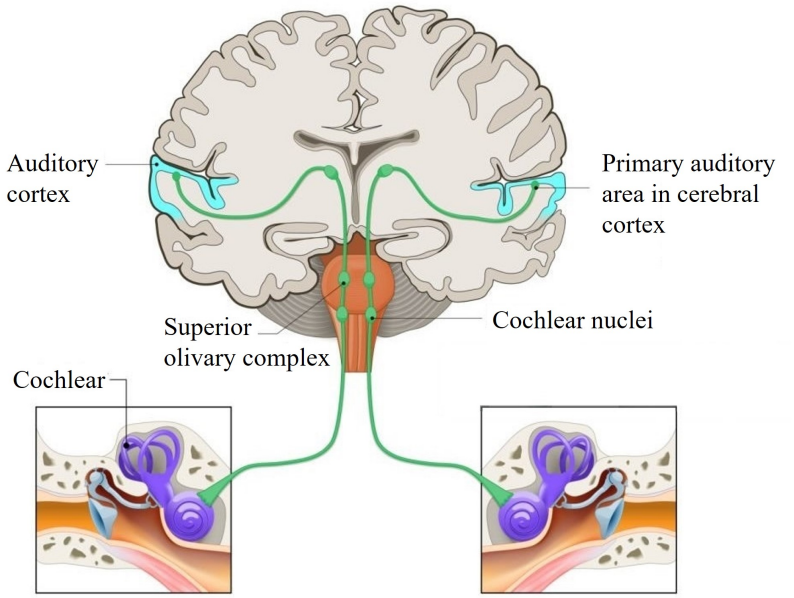

Fig. 1.11 Auditory pathways.

a specific band within the electroencephalographic (EEG) signal. Different psychological states are indeed associated with distinct neuronal oscillation frequencies [33]:

- Delta (1-3 Hz): deep sleep;
- Theta (4-7 Hz): light sleep, creativity, slow brain activity, relaxation;
- Alpha (8-13 Hz): awake states, relaxation, meditation;
- Beta (14-30 Hz): alertness, concentration;
- Gamma (>30 Hz): anxiety, attention.

Consequently, BB can be used to impact a person's cognition, mood, anxiety [34], memory, attention [35], and they can even be employed to reduce stress levels [30].

1.6 State of the Art

Stress is a widely studied topic in the literature. Different studies offer various solutions for identifying stress levels. As already mentioned, the gold standard in this field is the measurement of cortisol levels in blood samples or in salivary samples. Konen Obayashi proposes the use of other biomarkers such as α-amylase, chromogranin A, and immunoglobulin A as salivary markers of stress [36]. However, it is not always practical to obtain salivary samples, and, above all, it is not possible to continuously obtain an updated estimate of stress levels over time [13]. For this purpose, it is useful to use biosignals, which allow for real-time estimates of stress levels, with all the limitations involved. This aspect is particularly important, as stress levels are subject to variation over time, even within seconds.

Among biosignals, the most commonly used to assess stress levels are: heart rate (HR) [37],[38], HRV [8],[10],[39], and electrodermal activity (EDA) [38],[40]. Another possibility is to detect stress through the morphologic variability of the ECG, that is used as a complementary metric of HRV [41]. Some studies also employ QT interval variability, T wave amplitude, and breath rate in addition to HRV [3]. The advantage of utilizing these signals, beyond the capacity to continuously update stress level estimates, lies in their practicality, as they can be acquired through wearable sensors, such as Empatica E4, used for research purposes [42]. In contrast to the mentioned studies, this work leverages the entire ECG waveform, extracting specific features derived from amplitude and intervals values, as will be detailed in Chapter 2.

Despite the potential of neurostimulation via BB for stress reduction, the existing literature includes several studies with ambiguous or inconclusive findings. The literature highlights the importance of assessing the subject's condition prior to the experiment, as states of anxiety, depression, and chronic stress could affect the stimulation, making it ineffective [43]. Moreover, the sample should be as homogeneous as possible in terms of age and psychosocial state, and it should have gender balance. Another factor to consider is the choice of the rest condition. Silence might not lead the subject to relax as intended, thus failing to distinguish between the stress and rest phases during the protocol. Consequently, this could hinder the ability to draw valid conclusions regarding the effectiveness of the stimulation [30]. With this type

of stimulation, the key point is to achieve brainwave entrainment. However, studies show that it is not always possible to reach this goal. There is a great variety in the designs, so it is possible that entrainment did not occur under specific conditions. The variety concerns the sample of subjects considered, the stimulation frequency used (different frequency bands have different entrainment capacities), the carrier tones employed, and the chosen control condition: some use pure tones, others use non-overlapping tones, monaural beats, or silence [31]. In most studies, entrainment is not empirically demonstrated, but it is assumed. This could explain the failure of some studies in achieving a specific goal using BB.

In this field, the literature lacks guidelines on stimulation durations. In some cases, subjects are exposed to repeated stimulations over time. For instance, in [44], subjects are exposed to BB for 30 minutes for three consecutive evenings over four weeks. In [43], the stimulation duration is 15 minutes during the day and 30 minutes in the evening over a period of three weeks. In the case of [45], participants undergo stimulation for at least 10 minutes a day for one month. Other studies, on the other hand, employ shorter stimulation times, concentrated within the duration of the experimental protocol. One example is Hautus et al.'s work, that involves exposure to a stressor for 2 minutes, alternated with 4-minute recovery periods during which the stimulation is applied [30]. Seifi Ala et al. demonstrated that at least 9 minutes of stimulation are necessary to entrain the brain at a frequency in theta band [46], while Chockboondee et al. claim that a minimum of 4 minutes of stimulation in theta band is sufficient to increase parasympathethic activity, thus decreasing stress [45].

In general, in studies using BB for stress reduction, a stressor is included, but only in the case of a single-session study. To test the effectiveness of the stimulation in protocols that last for several days, the stress-inducing agent is not used. Normally, the duration of the exposure in a single session ranges from 5 minutes to 24 minutes [47].

In experimental protocols that involve the use of a stressor, stimulation is typically administered either before or after exposure to the stress-inducing agent. However, in some instances, stimulation is applied during the execution of the stress-inducing task [48]. This is the adopted approach in the present study.

One of the variables to consider in a protocol involving the use of BB is the possibility of overlaying the stimulation with noise. Various approaches have been investigated in this context, including pink noise [49],[46], Gaussian noise [50], and brown noise [51]. Some studies alternate between phases of stimulation with noise overlay and phases of noise alone to prevent habituation to the stimulation [46]. Conversely, other studies maintain the noise throughout the entire duration of the stimulation [51]. The rationale for incorporating noise with BB is that it serves to enhance their perception [32]. In this study, however, the aim is to reduce stress, and therefore the subject should not experience any discomfort when listening to BB. For this reason, the BB must be almost imperceptible, and no noise overlay is employed to emphasize them.

For stress reduction, the stimulation frequencies utilized lie within the theta and alpha bands, that are associated with relaxation [52]. When stress is induced, indeed, the alpha power in the cerebral cortex decreases [53]. It has been demonstrated that BB in theta band increase parasympathetic activity [44]. In addition to that, stimulating in this range of frequencies leads to an increase in the alpha power [46].

1.7 Objective of the Current Study

This study aims to design a closed-loop system that modulates BB stimulation in real-time to mitigate detected stress levels. Given the contradictory results available in literature, it is hypothesized that an optimal stimulation frequency exists for each individual, facilitating brainwave entrainment in the shortest possible time. By adapting the frequency to the subject, it is assumed that it is possible to overcome the inertia imposed by the central nervous system (CNS) more efficiently than with fixed-frequency stimulation. To achieve this, three key steps are involved:

1. Design of a stress inducing protocol.
2. Development of a model that can estimate stress levels in real time.
3. Implementation of a method for dynamically adjusting the stimulation frequency based on the real-time stress estimates.

Chapter 2

Materials and Methods

The aim of this chapter is to detail the procedure undertaken to accomplish the objectives set forth in the preceding chapter. It will outline the experimental protocol, along with the instrumentation and processing techniques employed.

2.1 Materials

For the execution of the experimental protocol, the following equipment is used:

- Beats Studio Buds + headphones with active noise canceling: utilized to provide auditory stimulation.
- Polar H10 Heart Rate Sensor: employed to acquire the ECG.
- hp laptop computer: used to receive and process data, and to display the protocol interface. It has a Windows 10 operating system, an i5 processor, and 8 GB of RAM.

Polar H10 is a highly accurate HR sensor. It consist of a chest strap with integrated electrodes for HR detection and a transmitter that sends the signal to the receiving device (Fig. 2.1). Polar H10 connects and transfers data via Bluetooth® and ANT+™. The HR monitor operates within a temperature range of -10 °C to 50 °C, has a sampling frequency of 130 Hz, and uses OwnCode® coded transmission (transmission of a unique signal recognized only by the associated receiver) [54].

Fig. 2.1 Polar H10 chest strap.

2.2 Participants

Eighteen healthy, young adults (23.2 $\pm$ 2.1 years old, 11 women and 7 men) participated in the present study. Subjects were instructed to refrain from engaging in physical activity, smoking, eating, and consuming caffeine, alcohol, or other stimulants during the three hours preceding the experiment. All data collection took place between 11:00 a.m. and 3:00 p.m. to minimize the potential influence of the circadian cycle on stress levels, as cortisol levels are typically higher in the morning upon waking and in the evening. All participants were fully informed about the purpose and procedures of the study and provided their consent to participate.

Particular attention was placed on the age of the participants. Age is a factor that affects hearing and, consequently, the perception of the auditory stimuli [46]. For this reason, the selected age range is between 19 and 30 years. All subjects possess an education level equal to or higher than a high school diploma. Additionally, they all confirmed their understanding of the English language, which was useful during the completion of the questionnaires.

An additional factor considered in the selection of subjects is body weight, as individuals with overweight conditions exhibit both hypo- and hyper-activation of the HPA axis. Similarly, underweight individuals demonstrate a higher cortisol awakening response compared to those with normal weight [55]. Furthermore, the ECG of overweight individuals exhibits alterations compared to the ECG of individuals with normal weight, including a leftward shift of the electrical axis, changes in P wave morphology, and an elongation of the QT interval [56].

2.3 Experimental Protocol

The protocol is conducted in a closed, quiet environment with white walls for neutral perceptions of emotion and mood [57]. Upon arrival, each subject is afforded time

to acclimate to the laboratory environment [8], as the prospect of participating in an experiment frequently induces a state of anxiety. Subsequently, participants are provided with questionnaires to complete.

2.3.1 Questionnaires

Pre-protocol questionnaires: assessing baseline metrics

Prior to the start of the protocol, each participant completes three questionnaires:

- **General Data**: used to gather information about the subject's habits, such as the consumption of stimulants, engagement in physical activity, hours of sleep prior to the protocol, medication intake, and overall health status. Information such as height, weight, and age is also requested in this questionnaire [55].
- **STAI** (Stress-Trait Anxiety Inventory): employed to assess the subject's current stress and anxiety levels through a set of 20 questions. Low anxiety levels correspond to a STAI score between 20 and 37, moderate levels fall within the range of 38 to 44, and high anxiety is indicated by scores from 45 to 80 [58].
- **PSS** (Perceived Stress Scale): utilized to assess the subject's stress levels over the past month, employing 10 questions. Scores between 0 and 13 indicate a low level of stress, scores between 14 and 26 indicate a moderate level, and scores between 27 and 40 indicate a high level of stress [59].

The literature recommends the use of at least two questionnaires for stress levels evaluation in order to obtain a more comprehensive picture of the subject's condition [55].

In-protocol questionnaires: real-time stress evaluation

During the experimental session, participants complete questionnaires assessing self-reported stress levels, using a Visual Analogue Scale (**VAS**) ranging from 0 to 5. Here, 0 indicates a state of relaxation, while 5 represents a high level of stress (Fig. 2.2).

Fig. 2.2 Intra-task questionnaire designed to assess the stress level perceived by the participant.

Post-protocol questionnaires: evaluating overall experience

Upon completion of the protocol, subjects are administered the NASA Task Load Index (**NASA-TLX**) questionnaire for measuring the mental workload through a series of six questions. Mental workload is categorized as follows: low (scores 0–9), medium (scores 10–29), somewhat high (scores 30–49), high (scores 50–79), and very high (scores 80–100) [60]. This approach aligns with guidelines that recommend monitoring the participants' mental state after the experiment as well [55].

2.3.2 Hearing Threshold Assessment

After the completion of the initial questionnaires, participants are instructed to sit comfortably at their workstation and wear the headphones.
Firstly, their hearing ability is tested using [61], evaluating each ear separately. Subsequently, their hearing threshold is assessed. The hearing threshold is the lowest intensity of a stimulus at which the subject first perceives sound. To perform this test, the subject is presented with a binaural tone at a specific frequency (6 Hz), which will be the same used during the fixed-frequency stimulation, that will be explained later. The volume level is set to 50% of the laptop's full range for all participants. From this level, the volume is decreased in 10 dB steps until the subject reports no longer hearing the stimulus. The stimulus intensity is then gradually increased in 5 dB steps until it becomes audible. At least two repetitions of this procedure are needed. If the intensity values obtained from the two repetitions differ, the test must be repeated until the same threshold is reached in at least half of the repetitions [62].

The auditory threshold is useful to ensure that the sample has homogeneous hearing abilities.

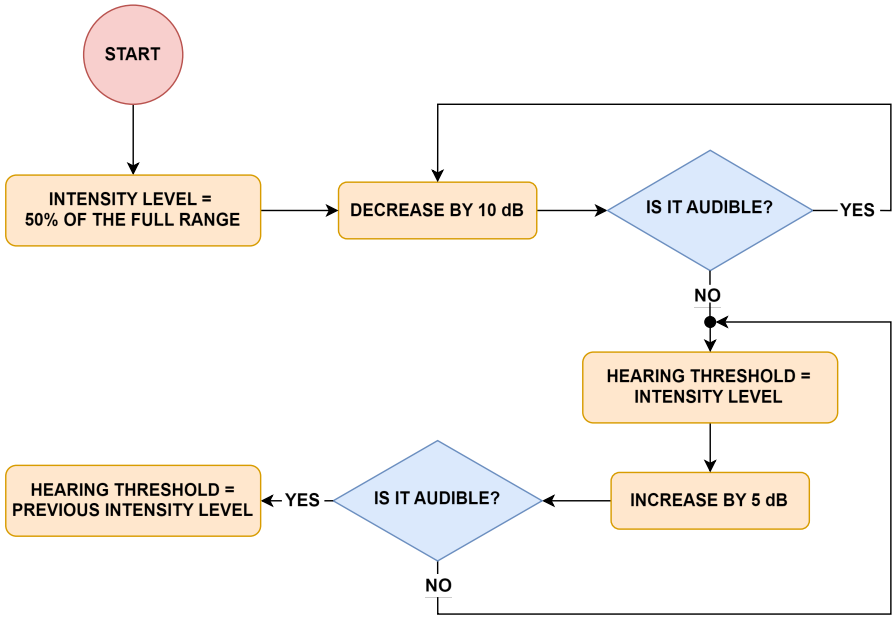

Fig. 2.3 Flowchart of the hearing threshold assessment procedure.

2.3.3 Stress Inducing Protocol

Throughout the entire protocol, the subject's ECG is recorded. First, the volunteer is fitted with the Polar strap, and then instructed to adjust the screen brightness and position according to their personal preferences.
Before wearing the chest strap, it is necessary to moisten the electrodes to improve contact with the skin and reduce the skin-electrode impedance. Subsequently, the elastic is secured around the subject's chest and adjusted according to their anthropometric measurements, ensuring it adheres properly to the skin and remains comfortable.

The tool used in the present study to induce stress is the mental arithmetic task. The subject is informed about the type of test they are required to perform. They are instructed to do their best and aim for the highest possible score, as they are participating in a competition. It has indeed been shown that competition and comparison with others are stress-inducing factors [55]. The results will be disclosed to them only upon the completion of the protocol.

Before the actual protocol begins, the subject undergoes a training phase in which the mathematical task to be performed is simulated. This allows them to familiarise themselves with the interface.

The protocol is divided into two parts. The first part serves to collect data to train the ML algorithm. The procedure begins with a white cross on a black background, shown for 2 seconds to capture the subject's attention [63]. This is followed by a 2-minute baseline period, during which the subject watches a video featuring natural landscapes and sounds, as these help to promote relaxation [64]. At the end of the video, the subject is asked to select their perceived level of stress on the VAS displayed, using the touchpad. Subsequently, the first mathematical task begins, lasting 4 minutes. During this phase, no stimulation is provided to the subject. The subject listens to relaxing music during the task, which will also be employed in the second part of the protocol to mask stimulation. To make the task even more stressful, the subject is given the impression of being recorded, and is informed that the recordings will later be reviewed and evaluated by experts [55]. At the end of the task, the participant is again asked to select their perceived level of stress. With the completion of the first mathematical task, the initial phase of the protocol concludes. The subject is permitted to relax and step away from the station if necessary. During this intermission, the ML model is trained.

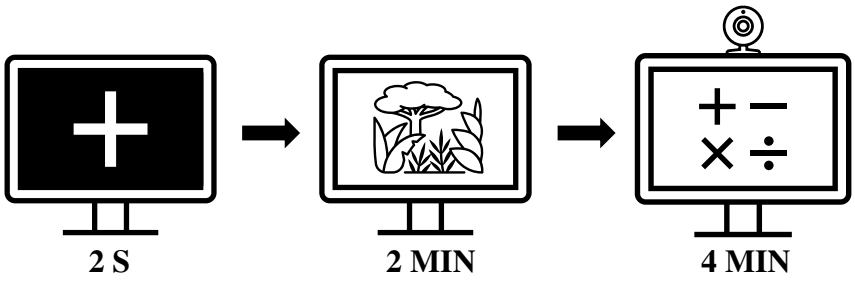

Fig. 2.4 Schematic representation of the first part of the protocol.

In the second phase, the trained model is applied to estimate stress levels in real time. This part of the protocol is structured as the previous one, but it includes two arithmetic tasks, during which the subject undergoes brainwave stimulation. These tests are alternated with periods of rest. As previously mentioned, during the arithmetic test, the subject is given the impression of being videotaped. At the beginning, a white cross is displayed for 2 seconds, followed by a 2-minute relaxing video with a natural theme. Subsequently, the second mathematical task

begins, lasting 4 minutes, after which there is a 2-minute rest period during which the subject views another nature-themed video. This is followed by the administration of the third mathematical test, also lasting 4 minutes. Similarly to the first part of the protocol, at the conclusion of each video or mathematical test, the VAS is presented on the screen for the subject to indicate their perceived stress level. At the conclusion of the protocol, the completion of the NASA-TLX questionnaire is required. Subsequently, the participant is informed of their performance, made aware that no video recordings were made, and is formally thanked and dismissed.

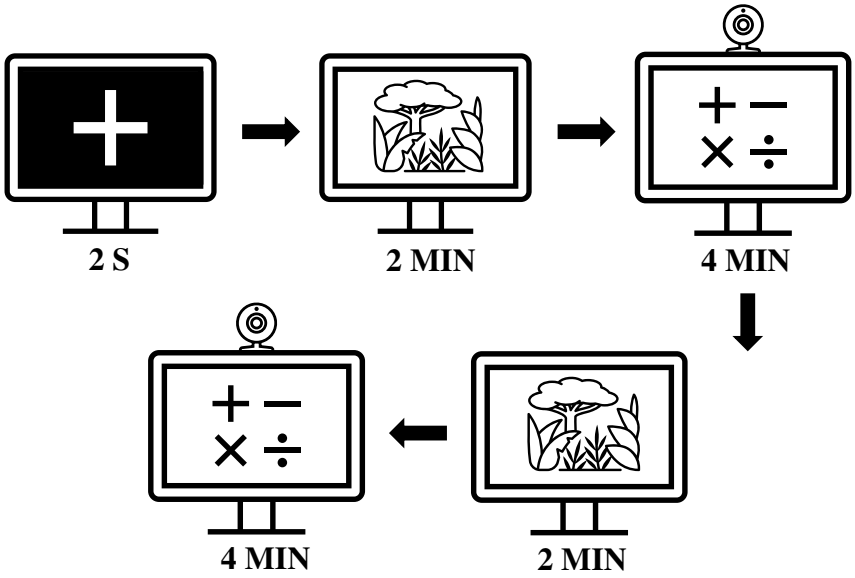

Fig. 2.5 Schematic representation of the second part of the protocol.

Mental Arithmetic Task

In this study, the quizzes are presented as open-ended questions. The subject is required to enter their answer in the designated box by typing it on the numeric keypad and pressing the enter key to confirm (Fig. 2.6). To increase the difficulty of the test, the subject is not allowed to use the backspace key, which is disabled. As a result, the first answer entered is considered final.
Each test consists of 60 questions. Each question is structured as follows:

$$N_1 \,\text{operator}\, N_2 = \text{Result}$$

where N_1, N_2, and Result are integers of at most 2 digits, while operator is one among the operators of addition, subtraction, multiplication, and division (+, -, *, /). Every quiz is randomly generated, and the seed selected for this purpose is set to 8. Depending on the type of operation, N_1 and N_2 can assume different values within a carefully selected range, designed to make the questions challenging but not overly difficult. Otherwise, there is a risk that the subject may become discouraged and abandon the problem without attempting to solve it. To structure the problems, the following rules are observed:

- In the case of single-digit numbers, the selected range is 3-9.
- In the case of addition or subtraction problems, if one between N_1 and N_2 is a single digit number, the other must have at least 2 digits.
- In the case of multiplication problems, only one between N_1 and N_2 can be a two-digit number, and in this scenario it can assume all the integers values in the range 10-20.
- In the case of division problems, N_2 is always a single-digit number, while N_1 is derived from the multiplication between N_2 and an integer number in the range 3-10.

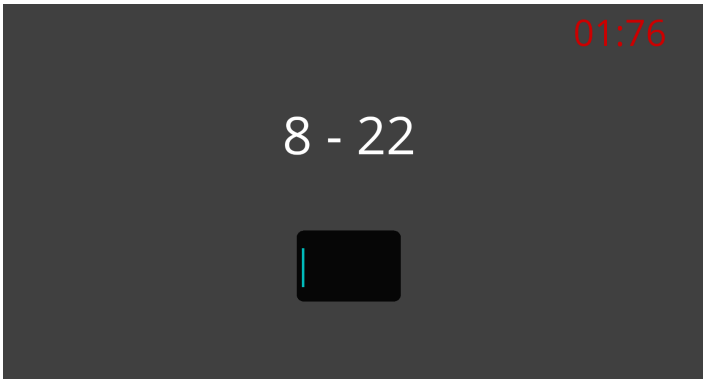

Fig. 2.6 Protocol interface displayed on the computer.

Tests have a specific percentage of addition, subtraction, multiplication, and division problems. The percentage for each type of operation is set at 20%, 30%, 20%, and 30%, respectively. The sequence of operations in each test does not adhere to a specific order of difficulty, and the types of operations are distributed throughout the entire set of questions. Another constant in the tests is the order of the types of

operations. For instance, if the first expression in the first test is an addition between a two-digit number and a one-digit number, the same applies to the first expression in the other two tests, and so on. This allows for an effective comparison of the three stimulation conditions (none, fixed, and adaptive) during the task's execution.

The subject has 4 seconds to answer each question. Response times for each question are recorded, along with the type of response given (correct, incorrect, or not given). The only feedback provided to the subject occurs in the event of an error, where the message "Incorrect answer!" is displayed, or in the case of an unanswered question, where the corresponding message appears. The subject is not informed of their score during the task.

Brainwave Stimulation

During the execution of the mathematical tests, the subject listens to relaxing music, which serves to mask the stimulation.
A signal-to-noise ratio (SNR) is established, defined as follows:

$$SNR_{\text{dB}} = 10 \cdot \log\left(\frac{P_{\text{BB}}}{P_{\text{music}}}\right)$$

where P_{BB} is the power of the BB (the signal), and P_{music} is the power of the music (the noise). The stimulation must be detectable by the participants but should not cause discomfort. For this reason, the SNR is set to -6 dB.
During these tests, stimulation is provided through BB in two distinct ways. In one test, the stimulation is delivered at a fixed frequency of 6 Hz, while in the other, the stimulation frequency is modulated based on the stress levels predicted by the ML model. For each participant, the order of the type of stimulation is randomly assigned, ensuring that half of the subjects are first exposed to fixed-frequency stimulation, while the other half are first exposed to adapted-frequency stimulation.

The order of stimulation is the only variable of the protocol among the various subjects. In fact, all participants undergo the exact same test without stimulation, and the same happens for those where the stimulation is applied. A specific test corresponds to the fixed-frequency stimulation, as it does for the adapted-frequency stimulation. The individual quizzes within a test are presented in the same order to all subjects.

2.4 Data processing

To train the ML algorithm, it is necessary to extract features from the ECG signal. To identify the waveforms within the ECG, the wavelet decomposition of the signal is performed using the Python package NeuroKit2 [65].
The signal is segmented with a variable length window based on the respiratory cycle. Specifically, a signal window corresponds to 3 respiratory cycles. The choice is driven by the fact that 3 is the minimum number of respiratory cycles that must be considered in order to perform the wavelet decomposition of the signal, as it would otherwise be insufficiently long. Moreover, 3 respiratory cycles correspond to an average of 12 seconds, a duration that aligns with the temporal lengths of the windows reported in the literature. The first step to be taken is therefore the extraction of the EDR signal from the ECG.

2.4.1 EDR Extraction

The initial step to be undertaken is the filtering of the ECG signal. The frequency band of the ECG is between 0.05 Hz and 150 Hz [66]. Given that the subjects perform minimal movements during the protocol, the effective bandwidth of the signal is between 0.05 Hz and 45 Hz. The ECG is then filtered using a 3^{rd}-order Chebyschev Type II high-pass filter, with a cutoff frequency of 0.05 Hz (Fig. 2.7 a)). Subsequently, the R peaks within the signal are identified utilizing the appropriate function in NeuroKit2 (Fig. 2.7 b)). By interpolating the R peaks using the Piecewise Cubic Hermite Interpolating Polynomial (PCHIP) technique, the EDR signal is derived (Fig. 2.7 c)) [22]. This signal is then subjected to filtering with a 5^{th}-order Butterworth low-pass filter at 0.5 Hz, followed by a 5^{th}-order Butterworth high-pass filter at 0.1 Hz (Fig. 2.7 d)) [20]. In the EDR signal, the peaks and valleys correspond to the onset of exhalation and inhalation, respectively. A respiratory cycle is arbitrarily defined as the signal occurring between two peaks, and consequently, between successive exhalations.

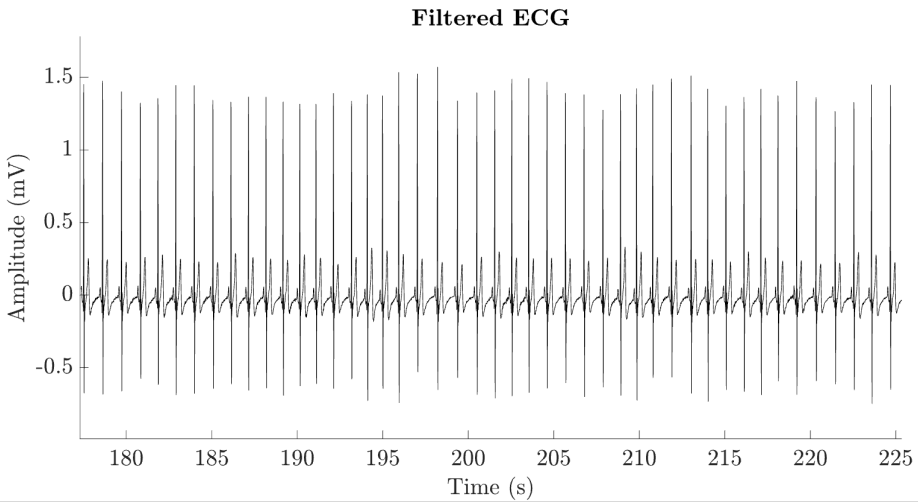
Filtered ECG
Amplitude (mV)
1.5
1
0.5
0
-0.5
180
185
190
195
200
205
210
215
220
225
Time (s)

a)

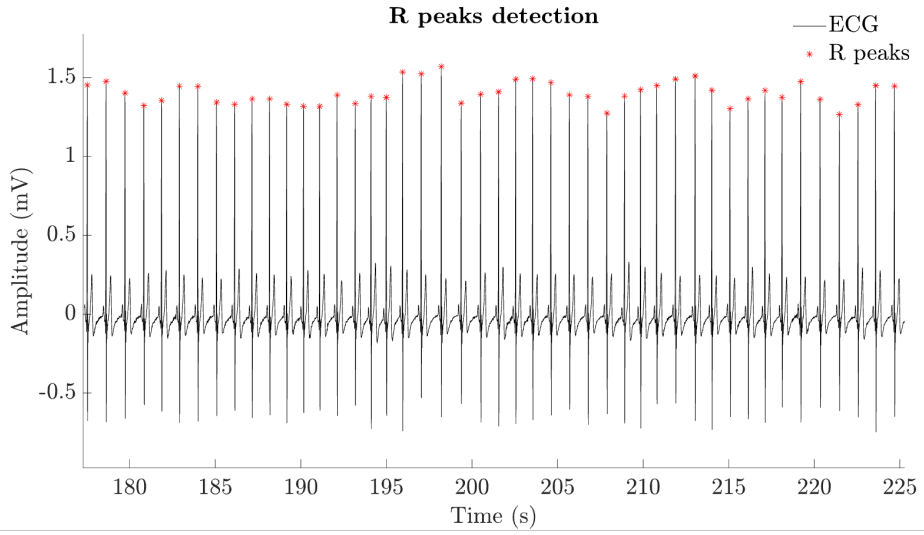
R peaks detection
ECG
R peaks
Amplitude (mV)
1.5
1
0.5
0
-0.5
180
185
190
195
200
205
210
215
220
225
Time (s)

b)

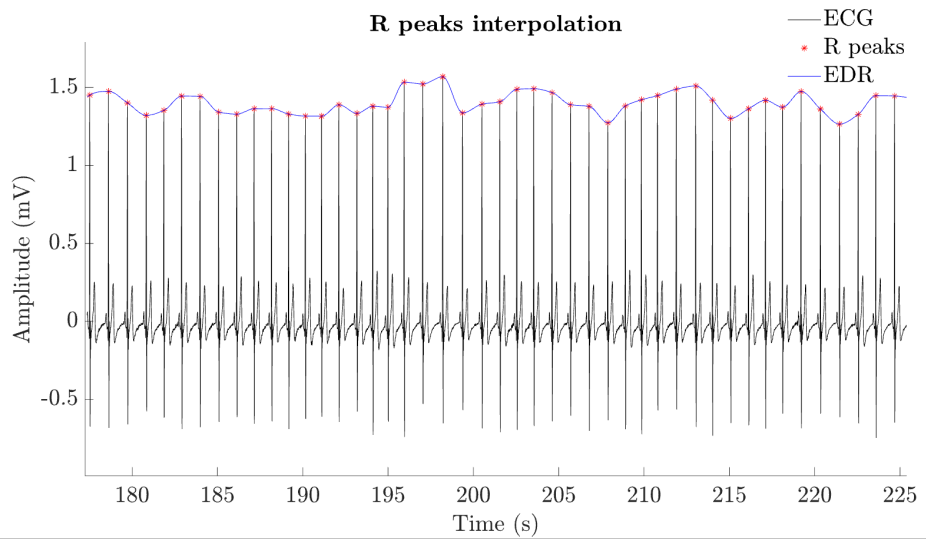

c)

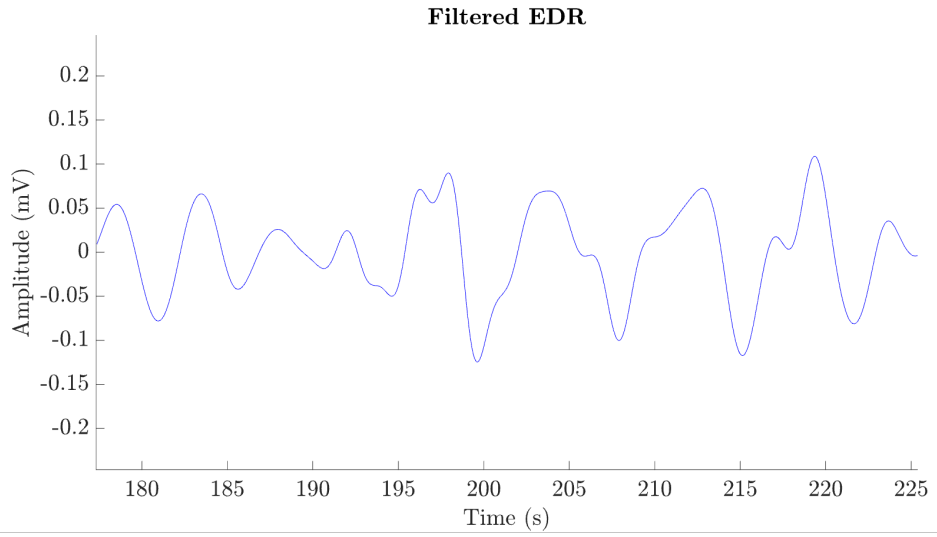

d)

Fig. 2.7 Processing steps. a) Filtered ECG. b) Identification of R peaks within the ECG. c) Interpolation of the R peaks. d) Filtered EDR.

2.4.2 Feature Extraction

For each signal window, a set of features is extracted. The mean value of each feature is calculated for every respiratory cycle within the window. As a result, 3 values are obtained for each feature. The feature set consists of:

- **RR interval**: defined as the interval between two consecutive R peaks.
- **QT interval**: defined as the interval between the the Q peak and the T peak within a single waveform.
- **QTc interval**: defined as the ratio between the QT interval and the square root of the RR interval.
- **RT ratio**: defined as the ratio between the R peak and the successive T peak.
- **RP ratio**: defined as the ratio between the R peak and the successive P peak.
- **BR ratio**: defined as the ratio between two consecutive peaks of the EDR signal.
- **BR width**: defined as the duration of a respiratory cycle.
- **BR pp**: defined as the ratio between a peak and the following valley of the EDR signal.

In addition to these, eight further features are included, that represent the change in the feature within the window across the various respiratory cycles. These features are derived by calculating the ratio of the feature value in the third respiratory cycle to those in the second and first respiratory cycles.

The features corresponding to the ECG signal acquired during the baseline are standardized using the StandardScaler algorithm from Python's scikit-learn library [67]. This algorithm normalizes the entire feature set, ensuring a mean of 0 and a standard deviation of 1. The standard score of a sample x is calculated as:

$$z = \frac{x - \mu}{\sigma}$$

where μ is the mean value of the feature set, and σ is the standard deviation. All subsequently extracted features related to the other sections of the protocol are normalized with respect to those of the baseline.

2.4.3 Model Training

A preliminary evaluation involves the application of two distinct ML models: the RF regressor and the SVR.
To identify the optimal regression model for each subject, a grid search algorithm is utilized. This approach enables the systematic evaluation of various parameter configurations and facilitates the identification of the optimal combination that results in the best model performance.
The method of cross-validation with 5 folds is employed. This entails dividing the data into 5 segments; the model is trained on 4 segments and tested on the remaining one. This process is repeated to ensure that each segment is utilized for testing. To evaluate performance, the coefficient of determination (R^2) is utilized for each iteration. The five R^2 coefficients are averaged to derive the metric that quantifies the model's goodness of fit. Finally, the model whose parameters provide the best mean R^2 is selected.

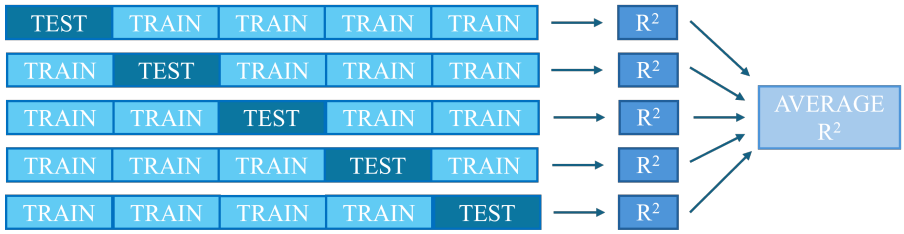

Fig. 2.8 Cross-validation procedure.

The hyperparameters used for the grid search are presented in the Table 2.1 for the RF algorithm, and in Table 2.2 for the SVR algorithm.

Table 2.1 Hyperparameters for grid search with RF regressor.

RF regressor	
Parameters	**Search values**
n_estimators	400, 700, 1000
max_features	None
max_depth	None, 10, 20, 30
min_samples_split	2, 5, 10
min_samples_leaf	2, 4, 6
bootstrap	True

Table 2.2 Hyperparameters for grid search with SVR.

SVR	
Parameters	**Search values**
kernel	linear, rbf, sigmoid
C	0.1, 1, 10
epsilon	0.1, 0.2, 0.5
gamma	scale, auto

Each model is trained for a specific subject using the following ground truth assignments:

- For features corresponding to the baseline condition, the label is assigned a value of 0, i.e. the relax state.
- For features corresponding to the arithmetic task, the label is assigned a value of 1, i.e. the stress state.

Upon the completion of the first mathematical task, an evaluation is conducted to verify the protocol's efficacy in inducing stress. The subject's responses to the questionnaire, where they report their perceived stress levels following both the video and the mathematical task, are compared to the ground truth. Given that the possible response values range from 0 to 5, the scores are rescaled as follows:

- 0, 1, 2 correspond to 0.
- 3, 4, 5 correspond to 1.

Following a performance assessment conducted on data from five subjects, the RF model is selected for the subsequent acquisition campaign. The results of these preliminary training sessions are reported in appendix A.

2.4.4 Real-Time Predictions

Once the model has been trained, it can be employed for real-time predictions of stress levels. The signal is segmented into windows corresponding to three respiratory cycles, from which feature values are extracted according to the procedure outlined

earlier. The regressor is then applied to the set of features, yielding three continuous outputs, each mapped between 0 and 1, one for each respiratory cycle. An overlap of two respiratory cycles is applied between consecutive windows (Fig. 2.9). As a result, for each respiratory cycle, a new output is derived, calculated as the average of the three predictions within the window.

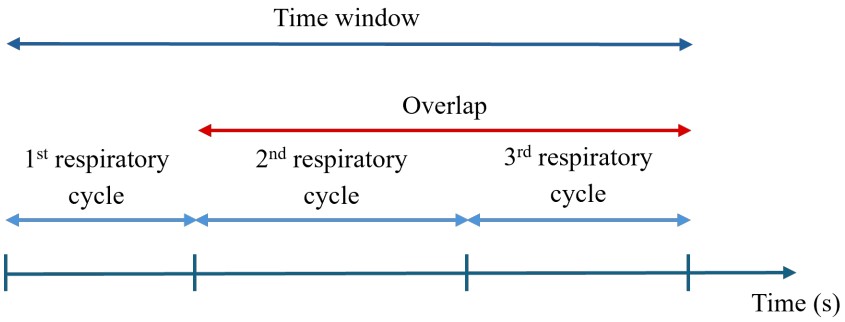

Fig. 2.9 Signal windowing.

2.5 Frequency Modulation Algorithm

The stimulation frequency through BB is modulated based on the stress level predicted by the regressor trained specifically for the individual subject. This frequency modulation is executed in real-time every four respiratory cycles. At each respiratory cycle, a prediction value is generated, and the modulation considers the last two predictions, corresponding to the most recent two respiratory cycles. The average of these two values is calculated to provide a more robust estimate of the subject's stress state during the latest time window. Only these two values are selected, as the initial two predictions are not deemed representative of the effects of the stimulation. The modulation is performed on the right channel of the headphones, while the left channel remains unvaried.

The underlying concept of the modulation involves seeking a minimum of a functional over time, described by the stress index predicted by the regressor. Let $I(f,t)$ represent the stress index, where f denotes the stimulation frequency, and t indicates time. For a brief period, such as the explored time window, it is assumed that variations in the stress index occur sufficiently slowly to justify the assumption

that I is solely a function of frequency. Consequently, the approximation $I(f,t) = I(f)$ can be adopted.

The selected frequency band is the theta band, encompassing frequencies ranging from 4 to 8 Hz. The procedure initiates with a frequency of 6 Hz, which corresponds to the stimulation frequency in fixed mode. Subsequently, the neighborhood of this frequency is explored with a 1 Hz step to assess how the functional varies over time. After the designated duration, the frequency is then adjusted to 5 Hz, and subsequently to 7 Hz.

With three prediction values corresponding to three stimulation frequencies, the minimum of the functional is sought. If this minimum is identified at 6 Hz, the surrounding area is investigated with a smaller step size, halving it at each iteration until reaching a minimum value of 0.125 Hz. Conversely, the preferred stimulation direction is determined: if the minimum is found at 5 Hz, the frequency will be decreased, while if it is located at 7 Hz, the frequency will be increased.

At this stage, the minimum of the functional is re-evaluated for the last two frequencies explored, in the direction considered correct. Subsequently, the neighborhood of the minimum is investigated once again, following the same procedure outlined previously. The algorithm iterates this process until the task is completed.

Prior to data acquisition from the subjects, the algorithm was tested on a simulated functional model representing the temporal evolution of the regressor [68]. Fig. 2.10 presents an example of a simulated functional, with the frequencies explored over a time interval comparable to the duration of the task in the experimental protocol. Ideally, in the final iteration, the algorithm would select a frequency corresponding to the global minimum of the functional. However, this outcome is not always achieved due to variations in the functional itself. Consequently, it is likely that the final frequency explored corresponds to a local minimum.

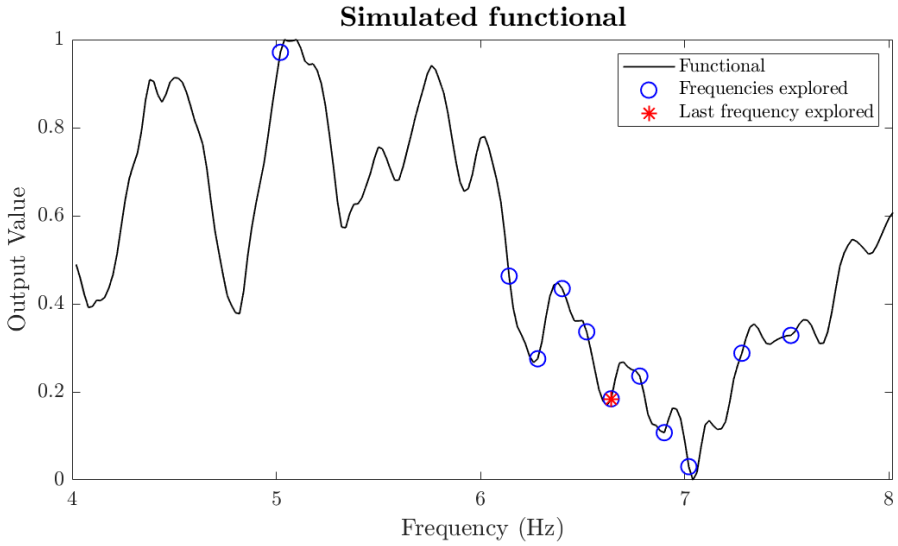

Fig. 2.10 Example of a simulated functional with the explored frequencies.

By modeling the behavior of the functional under the two conditions (fixed frequency and adapted frequency) according to the hypothesis that the adapted frequency is more effective in reducing the functional's value (Fig. 2.11), it is observed that a sufficiently large sample size (at least 30 subjects) is required to achieve strong statistically significant results.

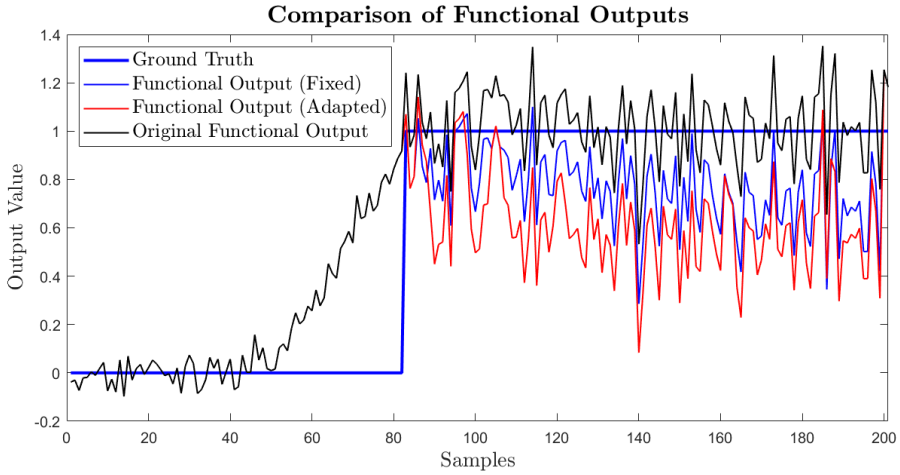

Fig. 2.11 Comparison of functional output among ground truth, original functional, functional after fixed-frequency stimulation, and functional after adapted-frequency stimulation.

In appendix B the flowchart of the frequency modulation algorithm is reported.

Chapter 3

Results

3.1 Demographic Profile of Participants

The demographic data for the entire sample is reported in table 3.1.
The study group is homogeneous regarding age (23.2 ± 2.1 years old), hours of sleep obtained the night prior to the execution of the experimental protocol (6.75 ± 1.13 hours), and auditory threshold (with a mean value of -47.22 dB). All participants possess a Body Mass Index (BMI) within the normal weight range [69], and their level of education is at least equivalent to a high school diploma.

Table 3.1 Demographic information for the sample. For Education Level (EL), HS denotes High School, while B refers to Bachelor. HT indicates the Hearing Threshold.

Demographic information						
Subject #	**Gender (M/F)**	**Age**	**BMI**	**Hours of sleep**	**HT (dB)**	**EL**
1	F	26	21.63	7.0	-50	HS
2	F	21	20.19	8.0	-55	HS
3	F	24	20.55	7.0	-60	B
4	F	21	20.07	6.0	-55	HS
5	M	28	24.62	8.0	-50	HS
6	F	24	23.22	6.0	-60	B
7	F	22	19.53	6.5	-55	HS
8	M	25	19.66	7.0	-40	B

Continued on next page

9	F	24	18.97	6.0	-50	B
10	M	25	22.50	6.0	-50	B
11	F	22	21.64	6.0	-50	HS
12	F	22	20.24	6.0	-55	HS
13	F	24	21.45	7.5	-50	B
14	M	20	21.25	7.0	-60	HS
15	M	20	21.84	8.0	-55	HS
16	F	23	22.09	9.0	-50	B
17	M	23	22.94	4.0	-55	HS
18	M	22	21.00	6.5	-50	HS

The sample exhibits a STAI score of 38.28 ± 10.14, indicating a moderate level of anxiety prior to the execution of the experimental protocol [58]. The mean PSS score is 22.50 ± 6.85, reflecting a moderate level of perceived stress experienced over the past month [59]. In contrast, the sample's NASA-TLX mean score is 58.07 ± 8.76, signifying a high level of mental workload associated with the protocol [60] (Fig. 3.1).

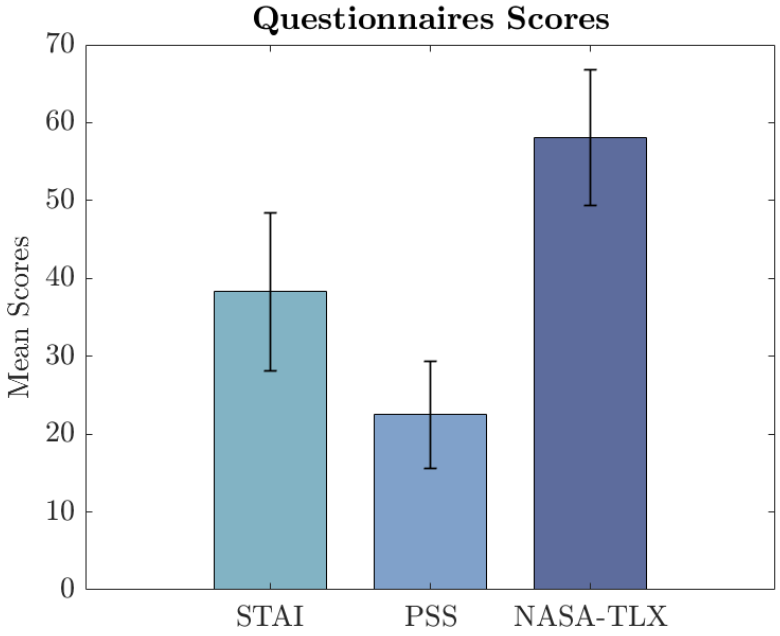

Fig. 3.1 Mean scores obtained from the STAI, PSS, and NASA-TLX questionnaires, with error bars representing standard deviation.

3.2 Assessing Protocol Effectiveness for Stress Induction

Prior to analyzing the data related to the effects of stimulation, it is essential to verify that the protocol has effectively induced stress in the participants. To this end, a comparison is made between the HR during the baseline period and that during the first arithmetic task. After testing the normality of the data distributions using the Lilliefors test, by performing the Wilcoxon signed-rank test, a $p < 0.001$ is obtained. Consequently, there exists a significant statistical difference between the two distributions of values, thereby confirming the efficacy of the mathematical test as a stress-inducing tool (Fig. 3.2). For comparison among more than two distributions of HR values, a repeated measures analysis of variance (ANOVA) is performed, yielding $p < 0.001$. Subsequently, the Wilcoxon test can then be conducted. No significant differences are found between the distributions of mean HR during the arithmetic test performed with fixed-frequency stimulation and that with adapted-frequency stimulation (Fig. 3.3).

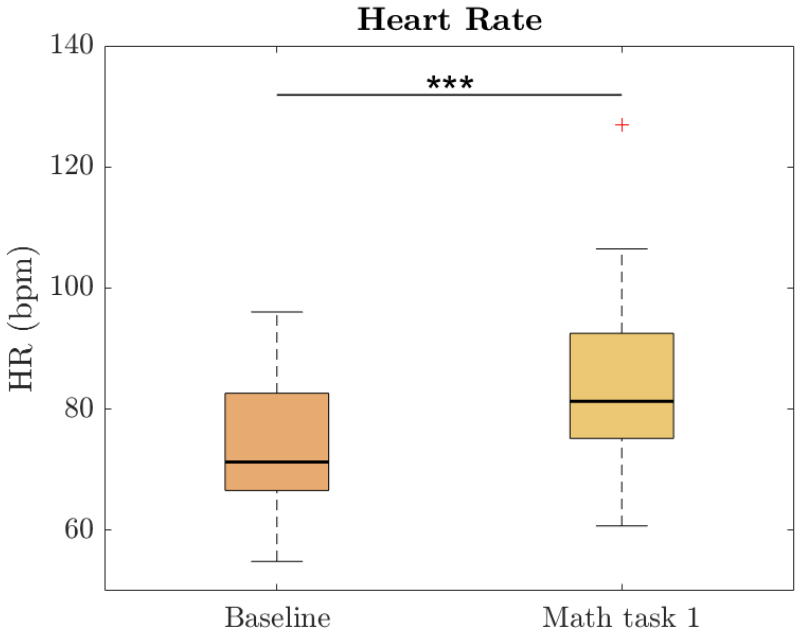

Fig. 3.2 Mean HR distributions during the Baseline and the first arithmetic task (Math Task 1) conditions. p-values indicate levels of statistical significance, with * indicating $p < 0.05$, ** indicating $p < 0.01$, and *** indicating $p < 0.001$.

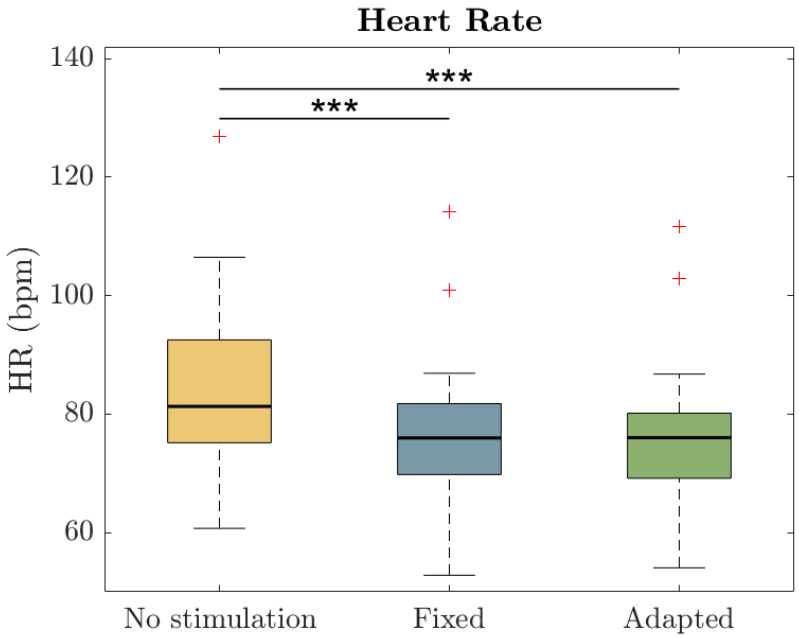

Fig. 3.3 Mean HR distributions during the three arithmetic tasks performed under the three conditions (No stimulation, Fixed, Adapted). p-values indicate levels of statistical significance, with * indicating $p < 0.05$, ** indicating $p < 0.01$, and *** indicating $p < 0.001$.

3.3 Performance Analyses

The performance on the mathematical tests is assessed. Specifically, the accuracy and the average reaction time are evaluated. The accuracy is defined as the percentage of correct responses for each test, while the average reaction time refers to the mean response time for questions answered correctly. Once the normality of the data distributions has been assessed using the Lilliefors test, a repeated measures ANOVA is conducted ($p < 0.001$). The distributions of these values are then compared across the test without stimulation, the test with fixed-frequency stimulation, and the test with stimulation adapted to stress levels. Significant differences are observed between the accuracy of the test conducted without stimulation and the accuracy of both tests where stimulation is applied ($p < 0.001$). In contrast, no significant differences are observed between the accuracy distributions of the test with fixed-frequency stimulation and the test with adapted-frequency stimulation.

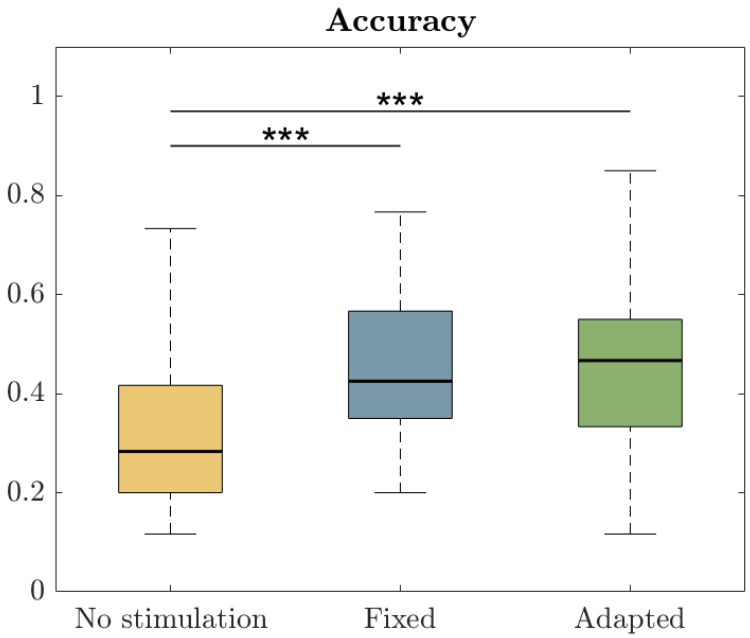

Fig. 3.4 Accuracy distributions for the arithmetic tasks conducted under the three conditions: no stimulation, fixed-frequency stimulation, and adapted stimulation. p-values represent the levels of statistical significance, where * denotes $p < 0.05$, ** denotes $p < 0.01$, and *** denotes $p < 0.001$.

No significant differences are found among the distributions of average reaction times (RT). Indeed, all statistical tests conducted between the different pairs of RT distributions indicate a $p > 0.05$ (Fig. 3.5).

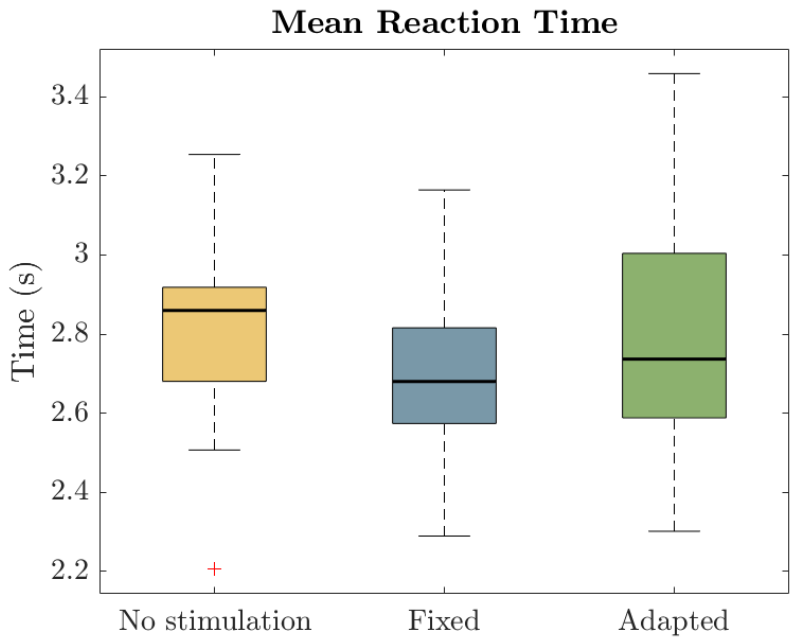

Fig. 3.5 Mean Reaction Time (RT) distributions for correct answers in the arithmetic tests conducted under the three conditions: no stimulation, fixed-frequency stimulation, and adapted stimulation.

3.4 Regressor Output Evaluation

The trend of the regressor is examined during the second part of the protocol, in which real-time predictions of the stress index are made. The Wilcoxon signed-rank test reveals a significant difference ($p = 0.022$) between the distribution of values associated with the regressor's average output during fixed-frequency stimulation and its average output during adaptive stimulation (Fig. 3.6).

Fig. 3.7 shows the distributions of responses to the VAS administered at the conclusion of each task in the protocol, in which participants indicated their perceived level of stress. The median of self-reported stress levels after adapted-frequency stimulation is lower than that after fixed-frequency stimulation.

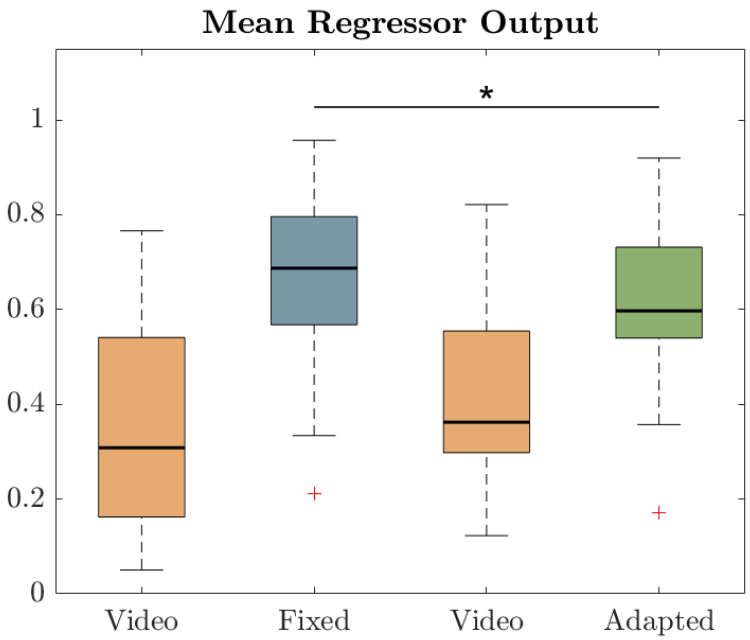

Fig. 3.6 Distributions of mean regressor output during the second part of the protocol. 'Fixed' and 'Adapted' refer to the arithmetic tests performed under the two stimulation conditions. p-values reflect the statistical significance levels, with * representing $p < 0.05$, ** representing $p < 0.01$, and *** representing $p < 0.001$.

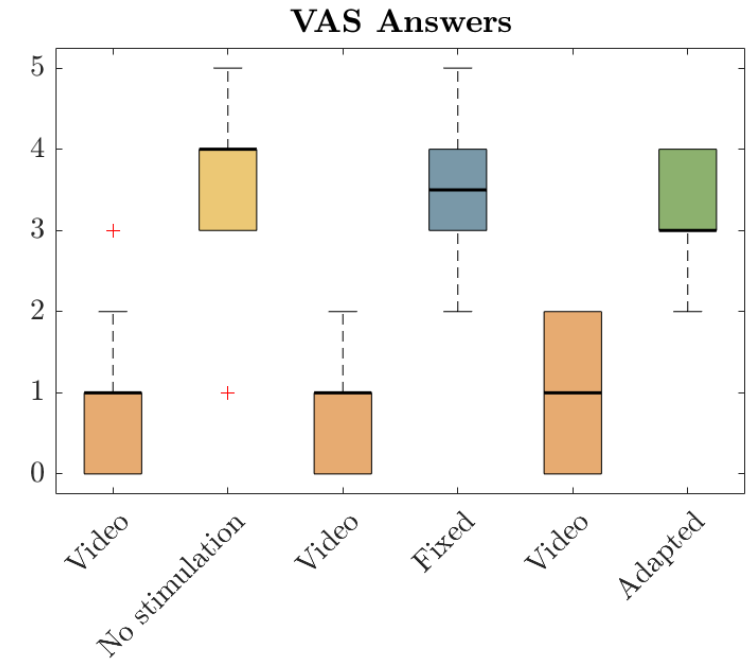

Fig. 3.7 Distributions of answers to the VAS shown after the completion of every task throughout the protocol.

To understand which features most significantly influenced the predictions of the regression model, the ranking of features, ordered by importance according to the RF algorithm, is presented. This ranking is obtained by averaging the importance value of each feature across all subjects. Notably, the RR interval emerges as the most informative feature with almost the 50% of importance, whereas features ranked below the fourth position exhibit a low importance value (Fig. 3.8).

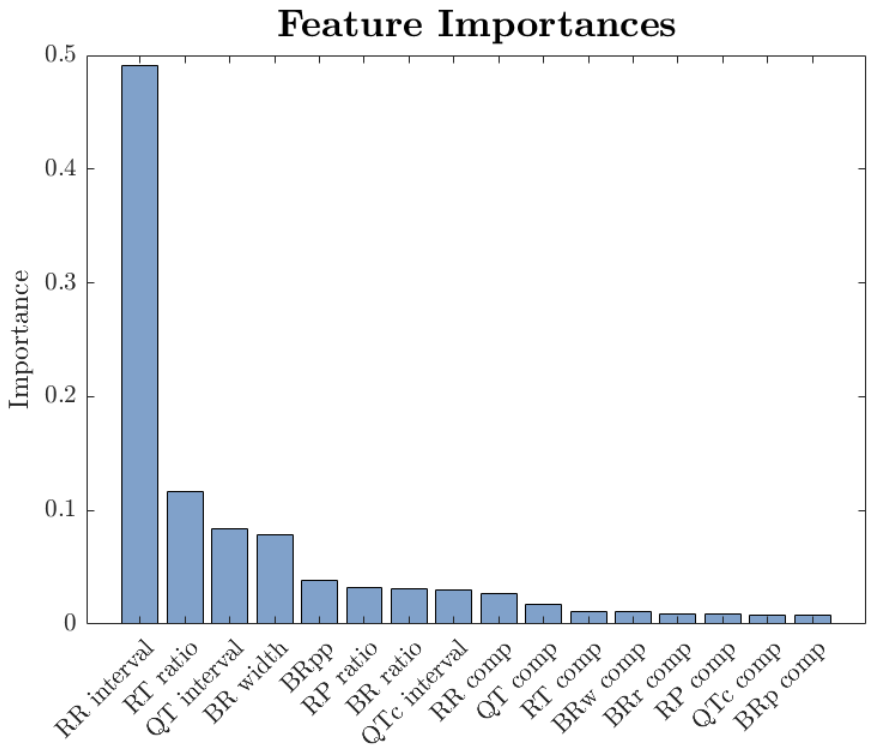

Fig. 3.8 Ranking of features by importance, from most to least influential in the model's predictions.

Although the RR interval is the most influential feature in predicting the model's output, it is not sufficient to distinguish between the stress and relaxation states. The distribution of its values, associated with the regressor's output during the task with adapted stimulation, does not clearly separate into the two classes, as illustrated in Fig. 3.9.

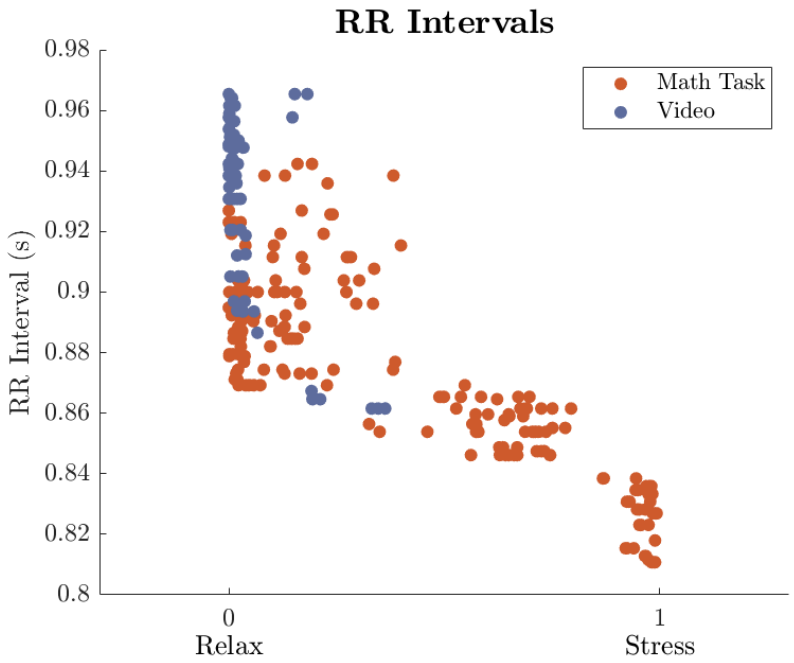

Fig. 3.9 Correlation between RR interval values and regressor's output for one subject during the task with adapted-frequency stimulation and the video preceding this task.

Chapter 4

Discussion

The analyses conducted on HR reveal significant differences between the value distributions associated with the baseline and the first arithmetic test. This finding suggests that the protocol is indeed effective in inducing stress in participants. Statistically significant differences are observed between HR data from the first arithmetic test, conducted without stimulation, and the test conducted with fixed-frequency stimulation. Similar observations apply to the comparison between HR data from the test without stimulation and that with adapted-frequency stimulation. This may be attributed to a reduced perception of stress in tests following the initial one. Conversely, no significant differences are found between the mean HR distributions for the two stimulation conditions, indicating that adapted-frequency stimulation does not yield improvements in terms of HR compared to fixed-frequency stimulation. Assuming that more stressful conditions are associated with higher heart rates than less stressful ones, a decrease in mean HR was expected during adapted stimulation compared to the fixed-frequency one.

Regarding performance, significant differences in accuracy are observed between the test conducted without stimulation and those conducted with stimulation. This variation may be attributable to a learning effect, and not to the stimulation per se. On the other hand, no differences are observed between the data from the two stimulation conditions, indicating no change in performance. As the stimulation was designed for stress reduction, and the two modalities were administered in random order, the lack of performance improvement in either the fixed-frequency condition or the adapted one is consistent with the intended goal. Achieving performance gains

would require frequencies within a different EEG band, such as the beta band, which promotes concentration.

The data concerning the mean RT for correct responses indicate no significant differences in any of the paired comparisons among the mathematical tests conducted under the three conditions (without stimulation, fixed-frequency stimulation, adapted-frequency stimulation). This can once again be explained by the fact that the frequencies employed are not designed to lead to an improvement in performance.

Although BB stimulation in the theta band does not yield performance benefits, a significant reduction in the mean value of the regressor's output is observed during user-adapted stimulation compared to the fixed-frequency one. This finding suggests that modulating the stimulation frequency according to the individual's stress level is more effective for stress reduction than the application of a fixed frequency. This outcome stands in contrast to the findings from HR analysis, indicating that HR alone may be insufficient to define a subject's stress level. Since the regression model is trained on a set of features derived from the full ECG waveform, this approach appears to offer a distinct advantage for stress assessment compared to methods that rely solely on HRV.

The benefits of adapted-frequency stimulation are also confirmed by participants' feedback collected through the VAS after each task. Overall, the perceived stress level during adapted-frequency stimulation is lower than that reported during fixed-frequency stimulation.

Based on the results obtained, it can be concluded that HRV alone is insufficient to describe a subject's stress level, contrary to what is stated in the literature. In fact, analysis of HRV data does not reveal any discernible differences between fixed-frequency and adaptive-frequency stimulation. The RF regressor utilizes all extracted features, assigning a ranking of importance according to each feature's influence on the prediction outcome. In most cases, with very few exceptions, the RR interval consistently ranks as the most significant feature. However, on average, the subsequent three features also receive a moderately high importance score, indicating that they provide informative contributions to the model's predictive accuracy. Conversely, features ranked below fourth in importance contribute minimally, and including them in the input only increases computational costs during both training and inference, without offering any substantial predictive advantage.

User-adapted stimulation shows some benefit in reducing stress, though its effect is minimal, typically manifesting as a slight reduction in the regressor's average output compared to that achieved with fixed-frequency stimulation. This limited impact may be influenced by several factors. First, BB are nearly imperceptible to the subject; as an auditory stimulus, they likely need to be distinctly audible to engage the CNS effectively. Additionally, administering stimulation during the arithmetic task may not be the optimal strategy for achieving this study's objectives. During the test, the subject's focus is on performing calculations rather than attending to the auditory input, potentially creating a conflict: the aim is to lower stress levels, yet the subject is simultaneously trying to excel at the task. Recent studies indicate that stimulation concurrent with cognitive tasks offers no added benefit; instead, pre-task stimulation appears to be more effective [70].

In light of these observations, a second data collection campaign was carried out to validate the conclusions drawn from this work. The methods and results of this additional data acquisitions are detailed in Chapter 5.

Chapter 5

Additional data acquisitions

5.1 Methods

For this data acquisition, eight subjects (five males and three females) are included, following the previous protocol with some modifications. Specifically, stimulation is administered prior to the arithmetic task. The task consists of open-ended questions involving only addition and subtraction of integer numbers, with a maximum of two digits. The experimental protocol is thus structured as follows:

1. 5 minutes of baseline, during which the subject listens to relaxing music with eyes closed.
2. 5 minutes of a math task without any background music.

Following these steps, the RF regression model is trained and subsequently used in the second part of the protocol to predict stress levels in real time. Given that only the top four features were relevant for algorithm training, the regressor is trained for each participant using only these highest-ranked features. Furthermore, the SNR between BB and music is set to -2 dB to enhance the perceptibility of the auditory beats. The protocol then proceeds with:

1. 5 minutes of stimulation with BB overlaid on music (either fixed or adaptive, chosen randomly), to be listened to with eyes closed.
2. 5 minutes of a math task without background music.

3. 1 minute of recovery.
4. 5 minutes of stimulation with BB overlaid on music (fixed or adaptive, the dual of the previous stimulation type), to be listened to with eyes closed.
5. 5 minutes of a math task without background music.

An additional difference from the previous approach lies in the processing method: the respiratory signal is estimated from the ECG using a specific function in the NeuroKit toolbox [65]. This toolbox employs the Van Gent method for extracting the EDR signal [71], utilizing a lower cutoff frequency for the low-pass filter (0.4 Hz) than the one previously utilized (0.5 Hz). With a cutoff frequency of 0.5 Hz, certain respiratory cycles were observed to be very short in duration, which limited the algorithm's ability to identify features within these signal windows due to insufficient data.

5.2 Results and Discussion

The sample is homogeneous in terms of age (23.9 ± 2.0 years old), hours of sleep obtained the night before the experimental protocol (6.8 ± 0.8 hours), and auditory threshold (with a mean value of -51.87 dB). All volunteers have a BMI within the normal weight range and an education level at least equivalent to a high school diploma.

Table 5.1 Demographic information for the sample. For Education Level (EL), HS denotes High School, B refers to Bachelor, and M refers to Master. HT indicates the Hearing Threshold.

Demographic information						
Subject #	**Gender (M/F)**	**Age**	**BMI**	**Hours of sleep**	**HT (dB)**	**EL**
1	F	24	19.10	6.5	-55	B
2	M	28	23.67	7.0	-50	M
3	M	24	20.18	8.0	-50	B
4	M	24	20.83	8.0	-55	B
5	F	22	22.77	6.0	-50	HS
6	M	21	20.52	7.0	-50	HS
7	F	24	18.75	6.0	-55	B
8	M	24	24.78	6.0	-50	B

The study group shows an average STAI score of 33.13 ± 5.38, suggesting a moderate level of anxiety before the experimental protocol [58]. The average PSS score is 16.13 ± 4.42, indicating a moderate level of perceived stress over the past month [59]. Conversely, the sample's NASA-TLX average score is 62.80 ± 12.10, reflecting a high level of mental workload related to the protocol [60] (Fig. 5.1).

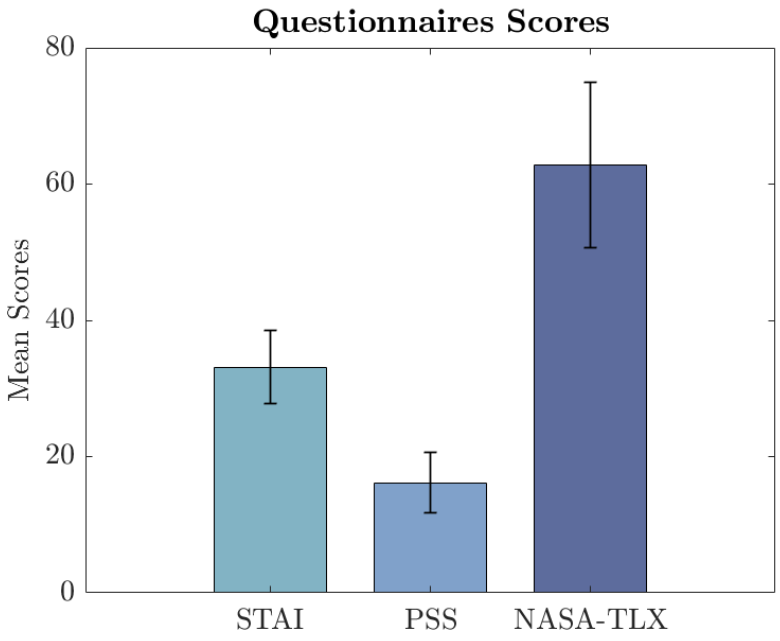

Fig. 5.1 Mean scores obtained from the STAI, PSS, and NASA-TLX questionnaires, with error bars representing standard deviation.

The distributions of the mean output values of the regressor across the protocol phases are shown in Fig 5.2. No statistically significant differences are observed between data associated with fixed-frequency and adaptive-frequency stimulation. However, a promising downward trend is observed between the mean output of the regressor during fixed-frequency stimulation and that during adapted stimulation. This lack of significance could be due to the limited amount of data, as eight subjects do not constitute a representative sample of the entire population.

Similarly, there are no differences between the average output during the task following fixed-frequency stimulation and the task following adaptive-frequency stimulation. The VAS responses support this finding (Fig. 5.3), as participants reported no perceived differences in stress levels between the conditions. This suggests that the mathematical test was conducted under comparable stress levels

after both stimulation types. The high cognitive load required by the test likely makes it unsuitable for evaluating stress reduction in response to stimulation designed for this purpose.

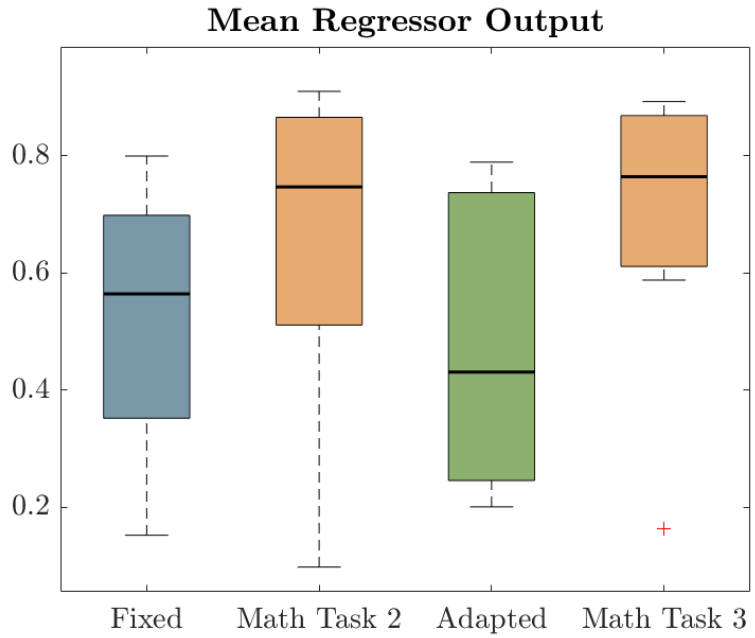

Fig. 5.2 Distributions of mean regressor output during the second part of the protocol. 'Fixed' and 'Adapted' refer to the two stimulation conditions.

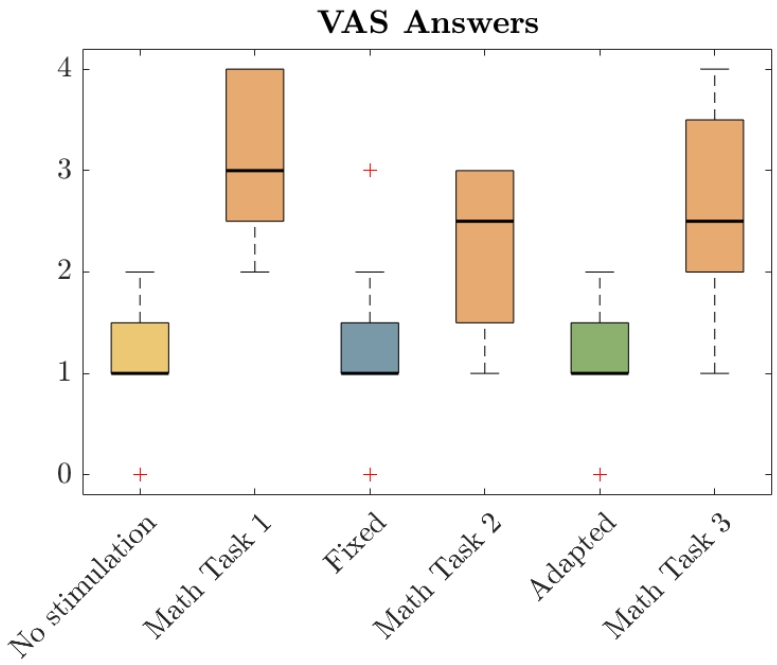

Fig. 5.3 Distributions of answers to the VAS shown after the completion of every task throughout the protocol.

5.3 Conclusion

Based on the results obtained from both experimental approaches, it can be concluded that the mathematical test is an effective stressor, but it is not the most suitable tool for assessing the stress index when auditory stimulation aimed at stress reduction is applied. Therefore, it may be useful to use this task only in the initial phase of the protocol to train the regression model. Subsequently, when the stimulation is administered, an alternative stress-inducing method could be employed, such as viewing a stressful video. This would prevent the conflict between the stimulation's purpose and the participant's goal of maximizing performance.

Despite this limitation, the regressor output results are promising, indicating that user-adapted stimulation in the theta band is more effective in reducing stress compared to the fixed-frequency stimulation at 6 Hz.

Based on the collected data, it is not possible to make a comparison between the two experimental approaches due to the differing number of participants included and to the use of the mathematical test during the stimulation phase of the protocol.

Consequently, it is not possible to determine whether it is more effective to administer stimulation before or during the task when the goal of the auditory beats is stress reduction. Nevertheless, both methods seem to support the initial hypothesis, as lower regressor output values are observed in tasks with modulated-frequency stimulation.

Further research is required to validate this assumption, involving a larger sample size and refining the protocol design based on the observations made in this study.

References

[1] Lindsay M Biga, Sierra Dawson, Amy Harwell, Robin Hopkins, Joel Kaufmann, Mike LeMaster, Philip Matern, Katie Morrison-Graham, Devon Quick, and Jon Runyeon. *Anatomy & physiology*. OpenStax/Oregon State University, 2020.

[2] Federico Vancheri, Giovanni Longo, Edoardo Vancheri, and Michael Y Henein. Mental stress and cardiovascular health—part i. *Journal of Clinical Medicine*, 11(12):3353, 2022.

[3] Hannes Ernst, Matthieu Scherpf, Sebastian Pannasch, Jens R Helmert, Hagen Malberg, and Martin Schmidt. Assessment of the human response to acute mental stress–an overview and a multimodal study. *PLoS One*, 18(11):e0294069, 2023.

[4] Maria Gardani, Daniel RR Bradford, Kirsten Russell, Stephanie Allan, Louise Beattie, Jason G Ellis, and Umair Akram. A systematic review and meta-analysis of poor sleep, insomnia symptoms and stress in undergraduate students. *Sleep medicine reviews*, 61:101565, 2022.

[5] Archana S Nagaraja, Nouara C Sadaoui, Piotr L Dorniak, Susan K Lutgendorf, and Anil K Sood. Snapshot: stress and disease. *Cell metabolism*, 23(2):388–388, 2016.

[6] Jonathan D Quick, Rebecca S Horn, and James Campbell Quick. Health consequences of stress. In *Job Stress*, pages 19–36. Routledge, 2014.

[7] Madhu Kalia. Assessing the economic impact of stress [mdash] the modern day hidden epidemic. *Metabolism-clinical and experimental*, 51(6):49–53, 2002.

[8] Santtu M Seipäjärvi, Anniina Tuomola, Joona Juurakko, Mirva Rottensteiner, Antti-Pekka E Rissanen, Jari LO Kurkela, Urho M Kujala, Jari A Laukkanen, and Jan Wikgren. Measuring psychosocial stress with heart rate variability-based methods in different health and age groups. *Physiological Measurement*, 43(5):055002, 2022.

[9] Jaap M Koolhaas, Alessandro Bartolomucci, Bauke Buwalda, Seitse F de Boer, Gabriele Flügge, S Mechiel Korte, Peter Meerlo, Robert Murison, Berend Olivier, Paola Palanza, et al. Stress revisited: a critical evaluation of the stress concept. *Neuroscience & Biobehavioral Reviews*, 35(5):1291–1301, 2011.

[10] Hye-Geum Kim, Eun-Jin Cheon, Dai-Seg Bai, Young Hwan Lee, and Bon-Hoon Koo. Stress and heart rate variability: a meta-analysis and review of the literature. *Psychiatry investigation*, 15(3):235, 2018.

[11] Patrice Boucher and Pierrich Plusquellec. Acute stress assessment from excess cortisol secretion: Fundamentals and perspectives. *Frontiers in endocrinology*, 10:749, 2019.

[12] Talha Iqbal, Adnan Elahi, William Wijns, and Atif Shahzad. Cortisol detection methods for stress monitoring in connected health. *Health Sciences Review*, 6:100079, 2023.

[13] Mouna Benchekroun, Dan Istrate, Vincent Zalc, and Dominique Lenne. Mmsd: A multi-modal dataset for real-time, continuous stress detection from physiological signals. In *HEALTHINF*, pages 240–248, 2022.

[14] Ibraheem Rehman and Afzal Rehman. Anatomy, thorax, heart. 2017.

[15] Dan B Tran, Carly Weber, and Richard A Lopez. Anatomy, thorax, heart muscles. 2019.

[16] C.L. Stanfield, W.J. Germann, M.J. Niles, and J.G. Cannon. *Principles of Human Physiology*. Pearson Benjamin Cummings, 2007.

[17] G.L. Cerone, M. Gazzoni, and M. Knaflitz. *Strumentazione biomedica*. Levrotto & Bella, 2022.

[18] Mario Merone, Paolo Soda, Mario Sansone, and Carlo Sansone. Ecg databases for biometric systems: A systematic review. *Expert Systems with Applications*, 67:189–202, 2017.

[19] Kejun Dong, Li Zhao, Cairong Zou, Zhipeng Cai, Chang Yan, Yang Li, Jianqing Li, and Chengyu Liu. A novel ecg-derived respiration method combining frequency-domain feature and interacting multiple model smoother. *IEEE Transactions on Biomedical Engineering*, 70(3):888–898, 2022.

[20] Axel Schäfer and Karl W Kratky. Estimation of breathing rate from respiratory sinus arrhythmia: comparison of various methods. *Annals of Biomedical Engineering*, 36:476–485, 2008.

[21] Lingeng Zhao, S Reisman, and T Findley. *Derivation of respiration from electrocardiogram during heart rate variability studies*. IEEE, 1994.

[22] Surita Sarkar, Saptak Bhattacherjee, and Saurabh Pal. Extraction of respiration signal from ecg for respiratory rate estimation. 2015.

[23] Sung-Bin Park, Yeon-Sik Noh, Sung-Jun Park, and Hyoung-Ro Yoon. An improved algorithm for respiration signal extraction from electrocardiogram measured by conductive textile electrodes using instantaneous frequency estimation. *Medical & biological engineering & computing*, 46:147–158, 2008.

[24] Jesús Lázaro, Alejandro Alcaine, Daniel Romero, Eduardo Gil, Pablo Laguna, Leif Sörnmo, and Raquel Bailón. Electrocardiogram derived respiration from qrs slopes: Evaluation with stress testing recordings. In *Computing in Cardiology 2013*, pages 655–658. IEEE, 2013.

[25] Batta Mahesh. Machine learning algorithms-a review. *International Journal of Science and Research (IJSR).[Internet]*, 9(1):381–386, 2020.

[26] Pekka Siirtola and Juha Röning. Comparison of regression and classification models for user-independent and personal stress detection. *Sensors*, 20(16):4402, 2020.

[27] Siddharth Bhalerao, Irshad Ahmad Ansari, and Anil Kumar. Reversible ecg data hiding: Analysis and comparison of ann, regression svm and random forest regression. In *2020 International Conference on Communication and Signal Processing (ICCSP)*, pages 0667–0671. IEEE, 2020.

[28] Brian CJ Moore. *An introduction to the psychology of hearing*. Brill, 2012.

[29] Hector D Orozco Perez, Guillaume Dumas, and Alexandre Lehmann. Binaural beats through the auditory pathway: from brainstem to connectivity patterns. *Eneuro*, 7(2), 2020.

[30] Michael J Hautus, Daniel Shepherd, Edmund Giang, and Jason Landon. Can binaural beats facilitate autonomic recovery following exposure to an acute stressor? *Complementary Therapies in Clinical Practice*, 45:101485, 2021.

[31] Ruth Maria Ingendoh, Ella S Posny, and Angela Heine. Binaural beats to entrain the brain? a systematic review of the effects of binaural beat stimulation on brain oscillatory activity, and the implications for psychological research and intervention. *Plos one*, 18(5):e0286023, 2023.

[32] Gerald Oster. Auditory beats in the brain. *Scientific American*, 229(4):94–103, 1973.

[33] Tina L Huang and Christine Charyton. A comprehensive review of the psychological effects of brainwave entrainment. *Database of Abstracts of Reviews of Effects (DARE): Quality-assessed Reviews [Internet]*, 2008.

[34] Leila Chaieb, Elke Caroline Wilpert, Thomas P Reber, and Juergen Fell. Auditory beat stimulation and its effects on cognition and mood states. *Frontiers in psychiatry*, 6:70, 2015.

[35] Sandhya Basu and Bidisha Banerjee. Potential of binaural beats intervention for improving memory and attention: insights from meta-analysis and systematic review. *Psychological Research*, 87(4):951–963, 2023.

[36] Konen Obayashi. Salivary mental stress proteins. *Clinica chimica acta*, 425:196–201, 2013.

[37] Tanja GM Vrijkotte, Lorenz JP Van Doornen, and Eco JC De Geus. Effects of work stress on ambulatory blood pressure, heart rate, and heart rate variability. *Hypertension*, 35(4):880–886, 2000.

[38] Tatyana Reinhardt, Christian Schmahl, Stefan Wüst, and Martin Bohus. Salivary cortisol, heart rate, electrodermal activity and subjective stress responses to the mannheim multicomponent stress test (mmst). *Psychiatry research*, 198(1):106–111, 2012.

[39] Juan Sztajzel. Heart rate variability: a noninvasive electrocardiographic method to measure the autonomic nervous system. *Swiss medical weekly*, 134(3536):514–522, 2004.

[40] Cheyenne Samson and Ahyeon Koh. Stress monitoring and recent advancements in wearable biosensors. *Frontiers in bioengineering and biotechnology*, 8:1037, 2020.

[41] Raritan Costin, Cristian Rotariu, and Alexandru Pasarica. Mental stress detection using heart rate variability and morphologic variability of eeg signals. In *2012 International Conference and Exposition on Electrical and Power Engineering*, pages 591–596. IEEE, 2012.

[42] Angela AT Schuurmans, Peter De Looff, Karin S Nijhof, Catarina Rosada, Ron HJ Scholte, Arne Popma, and Roy Otten. Validity of the empatica e4 wristband to measure heart rate variability (hrv) parameters: A comparison to electrocardiography (ecg). *Journal of medical systems*, 44:1–11, 2020.

[43] Minji Lee, Hyuk Joo Lee, Junseok Ahn, Jung Kyung Hong, and In-Young Yoon. Comparison of autonomous sensory meridian response and binaural auditory beats effects on stress reduction: a pilot study. *Scientific Reports*, 12(1):19521, 2022.

[44] MeLisa A Gantt, Stephanie Dadds, Debra S Burns, Dale Glaser, and Angelo D Moore. The effect of binaural beat technology on the cardiovascular stress response in military service members with postdeployment stress. *Journal of Nursing Scholarship*, 49(4):411–420, 2017.

[45] Mondnath Chockboondee, Tirapoot Jatupornpoonsub, Krisna Lertsukprasert, and Yodchanan Wongsawat. Long and short durations of binaural beats differently affect relaxation: a study of hrv and brums. *IEEE Access*, 2023.

[46] Tirdad Seifi Ala, Mohammad Ali Ahmadi-Pajouh, and Ali Motie Nasrabadi. Cumulative effects of theta binaural beats on brain power and functional connectivity. *Biomedical signal processing and control*, 42:242–252, 2018.

[47] Jennifer Platt and Lucy Hammond. Is non-clinical, personal use of binaural beats audio an effective stress-management strategy? a systematic review of randomised control trials. *Advances in Mental Health*, pages 1–29, 2024.

[48] Yara Badr, Fares Al-Shargie, Usman Tariq, Fabio Babiloni, Fadwa Al-Mughairbi, and Hasan Al-Nashash. Mental stress detection and mitigation using machine learning and binaural beat stimulation. In *2023 45th Annual International Conference of the IEEE Engineering in Medicine & Biology Society (EMBC)*, pages 1–5. IEEE, 2023.

[49] Patrick A McConnell, Brett Froeliger, Eric L Garland, Jeffrey C Ives, and Gary A Sforzo. Auditory driving of the autonomic nervous system: Listening to theta-frequency binaural beats post-exercise increases parasympathetic activation and sympathetic withdrawal. *Frontiers in psychology*, 5:1248, 2014.

[50] John H Grose, Emily Buss, and Joseph W Hall III. Binaural beat salience. *Hearing Research*, 285(1-2):40–45, 2012.

[51] Elizabeth Krasnoff and Gaétan Chevalier. Case report: binaural beats music assessment experiment. *Frontiers in Human Neuroscience*, 17:1138650, 2023.

[52] Kalle Jurvanen et al. Binaural beats and music: using theta and alpha waves in music to induce relaxation and meditation. Master's thesis, 2020.

[53] H Norhazman, N Mohamad Zaini, MN Taib, HA Omar, R Jailani, S Lias, Lucyantie Mazalan, and Maizura Mohd Sani. Behaviour of eeg alpha asymmetry when stress is induced and binaural beat is applied. In *2012 international symposium on computer applications and industrial electronics (ISCAIE)*, pages 297–301. IEEE, 2012.

[54] Polar. *Manuale d'uso: Sensore di frequenza cardiaca Polar H10*, 2024.

[55] NF Narvaez Linares, Valérie Charron, Allison J Ouimet, Patrick R Labelle, and Helene Plamondon. A systematic review of the trier social stress test methodology: Issues in promoting study comparison and replicable research. *Neurobiology of stress*, 13:100235, 2020.

[56] MA Fraley, JA Birchem, N Senkottaiyan, and MA Alpert. Obesity and the electrocardiogram. *Obesity reviews*, 6(4):275–281, 2005.

[57] Nantawachara Jirakittayakorn and Yodchanan Wongsawat. Brain responses to a 6-hz binaural beat: effects on general theta rhythm and frontal midline theta activity. *Frontiers in neuroscience*, 11:365, 2017.

[58] Ozcan Kayikcioglu, Sinan Bilgin, Goktug Seymenoglu, and Artuner Deveci. State and trait anxiety scores of patients receiving intravitreal injections. *Biomedicine hub*, 2(2):1–5, 2017.

[59] Karla Gambetta-Tessini, Rodrigo Mariño, Mike Morgan, Wendell Evans, and Vivienne Anderson. Stress and health-promoting attributes in australian, new zealand, and chilean dental students. *Journal of Dental Education*, 77(6):801–809, 2013.

[60] Atyanti Dyah Prabaswari, Chancard Basumerda, and Bagus Wahyu Utomo. The mental workload analysis of staff in study program of private educational organization. In *IOP Conference Series: Materials Science and Engineering*, volume 528, page 012018. IOP Publishing, 2019.

[61] Centro Audiologico Audire. Hearing test - test dell'udito audire di milano e lodi, 2014.

[62] Marcin Masalski. The hearing test app for android devices: distinctive features of pure-tone audiometry performed on mobile devices. *Medical Devices: Evidence and Research*, pages 151–163, 2024.

[63] Matti Gärtner, Simone Grimm, and Malek Bajbouj. Frontal midline theta oscillations during mental arithmetic: effects of stress. *Frontiers in behavioral neuroscience*, 9:133588, 2015.

[64] Jesper J Alvarsson, Stefan Wiens, and Mats E Nilsson. Stress recovery during exposure to nature sound and environmental noise. *International journal of environmental research and public health*, 7(3):1036–1046, 2010.

[65] Dominique Makowski, Tam Pham, Zen J. Lau, Jan C. Brammer, François Lespinasse, Hung Pham, Christopher Schölzel, and S. H. Annabel Chen. NeuroKit2: A python toolbox for neurophysiological signal processing. *Behavior Research Methods*, 53(4):1689–1696, feb 2021.

[66] Paul Kligfield, Leonard S Gettes, James J Bailey, Rory Childers, Barbara J Deal, E William Hancock, Gerard Van Herpen, Jan A Kors, Peter Macfarlane, David M Mirvis, et al. Recommendations for the standardization and interpretation of the electrocardiogram: part i: the electrocardiogram and its technology: a scientific statement from the american heart association electrocardiography and arrhythmias committee, council on clinical cardiology; the american college of cardiology foundation; and the heart rhythm society endorsed by the international society for computerized electrocardiology. *Circulation*, 115(10):1306–1324, 2007.

[67] F. Pedregosa, G. Varoquaux, A. Gramfort, V. Michel, B. Thirion, O. Grisel, M. Blondel, P. Prettenhofer, R. Weiss, V. Dubourg, J. Vanderplas, A. Passos, D. Cournapeau, M. Brucher, M. Perrot, and E. Duchesnay. Scikit-learn: Machine learning in Python. *Journal of Machine Learning Research*, 12:2825–2830, 2011.

[68] Lorenzo Bachi, Hesam Halvaei, Cristina Pérez, Alba Martín-Yebra, Andrius Petrėnas, Andrius Sološenko, Linda Johnson, Vaidotas Marozas, Juan Pablo Martínez, Esther Pueyo, et al. Ecg modeling for simulation of arrhythmias in time-varying conditions. *IEEE Transactions on Biomedical Engineering*, 70(12):3449–3460, 2023.

[69] HJOR Obese. Body mass index (bmi). *Obes Res*, 6(2):51S–209S, 1998.

[70] Miguel Garcia-Argibay, Miguel A Santed, and José M Reales. Efficacy of binaural auditory beats in cognition, anxiety, and pain perception: a meta-analysis. *Psychological research*, 83:357–372, 2019.

[71] Paul Van Gent, Haneen Farah, Nicole Van Nes, and Bart Van Arem. Heartpy: A novel heart rate algorithm for the analysis of noisy signals. *Transportation research part F: traffic psychology and behaviour*, 66:368–378, 2019.

Appendix A

Preliminary trainings

A.1 Subject 1

RF regressor	
Parameters	**Selected values**
n_estimators	700
max_features	None
max_depth	30
min_samples_split	2
min_samples_leaf	6
bootstrap	True
R^2	**0.98**

SVR	
Parameters	**Selected values**
kernel	rbf
C	10
epsilon	0.1
gamma	scale
R^2	**0.92**

A.2 Subject 2

RF regressor	
Parameters	**Selected values**
n_estimators	700
max_features	None
max_depth	None
min_samples_split	5
min_samples_leaf	2
bootstrap	True
R^2	**0.92**

SVR	
Parameters	**Selected values**
kernel	rbf
C	1
epsilon	0.1
gamma	scale
R^2	**0.86**

A.3 Subject 3

RF regressor	
Parameters	**Selected values**
n_estimators	400
max_features	None
max_depth	20
min_samples_split	5
min_samples_leaf	2
bootstrap	True
R^2	**0.92**

SVR	
Parameters	**Selected values**
kernel	rbf
C	1
epsilon	0.1
gamma	auto
R^2	**0.83**

A.4 Subject 4

RF regressor	
Parameters	**Selected values**
n_estimators	400
max_features	None
max_depth	20
min_samples_split	2
min_samples_leaf	2
bootstrap	True
R^2	**0.93**

SVR	
Parameters	**Selected values**
kernel	rbf
C	10
epsilon	0.1
gamma	scale
R^2	**0.84**

A.5 Subject 5

RF regressor	
Parameters	**Selected values**
n_estimators	400
max_features	None
max_depth	30
min_samples_split	5
min_samples_leaf	2
bootstrap	True
R^2	**0.92**

SVR	
Parameters	**Selected values**
kernel	rbf
C	10
epsilon	0.1
gamma	auto
R^2	**0.84**

Appendix B

Frequency modulation algorithm - Flowchart

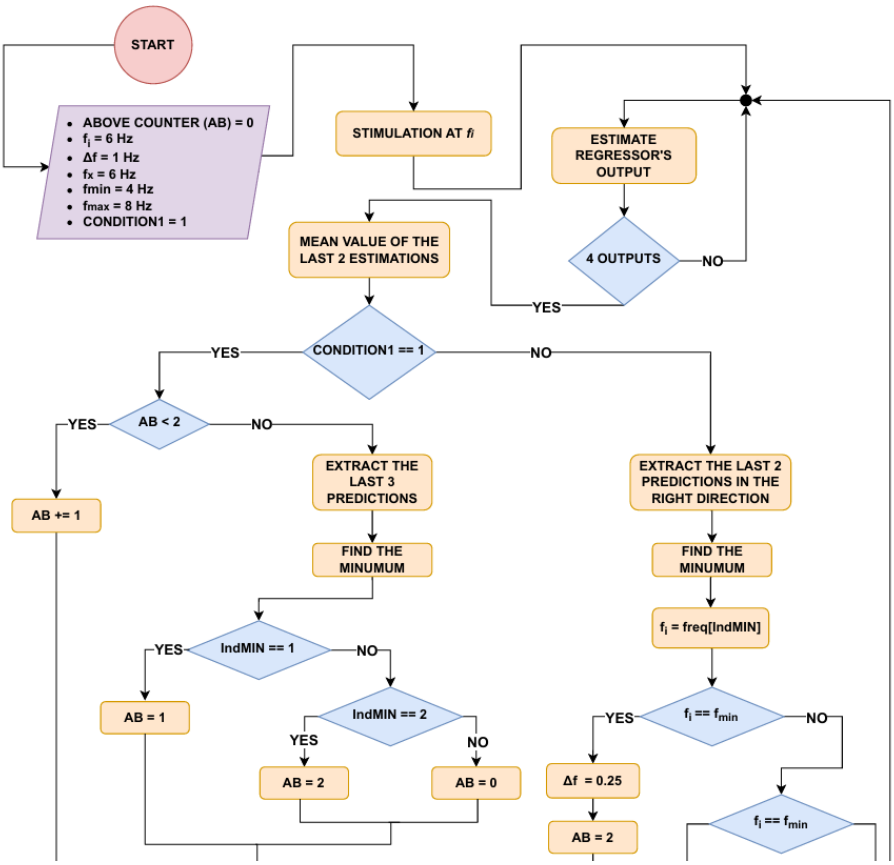

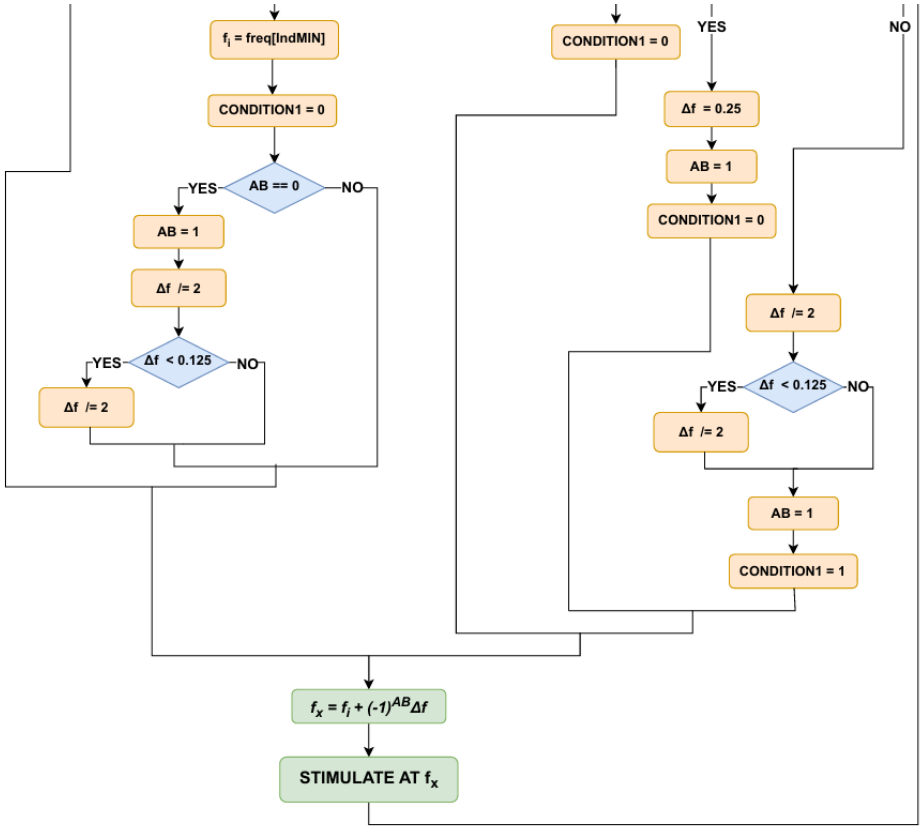
f_i = freq[IndMIN]
CONDITION1 = 0
AB == 0
YES
NO
AB = 1
Δf /= 2
Δf < 0.125
YES
NO
Δf /= 2
CONDITION1 = 0
YES
NO
Δf = 0.25
AB = 1
CONDITION1 = 0
Δf /= 2
Δf < 0.125
YES
NO
Δf /= 2
AB = 1
CONDITION1 = 1
$f_x = f_i + (-1)^{AB}\Delta f$
STIMULATE AT f_x